Lignin/Carbon Fibre Composites

Degree Project in Chemical Engineering and Technology,
First Cycle, 15 credits
KA103X

Authors:
Ali Al Husseinat
Ran Carlhamn Rasmussen
Emma Persson
Filip Rynkiewicz

Supervisor: Iuliana Ribca
Examiner: Mats Johansson

KTH Royal Institute of Technology
Department of Chemistry
Fibre and Polymer Technology

Stockholm, Sweden 2021

Abstract

The market is in great need of more environmentally friendly alternatives to fossil-based composite materials to obtain a more sustainable future. Lignin is the second most common biopolymer and is a byproduct in the pulping and paper industry. Fractionation of lignin has made it possible to receive lignin with narrow dispersity and low molecular weight, which is suitable for further applications. Modification of lignin structure yields new reactive sites that can be tailored for specific needs. Because of the aromatic structure of lignin, it is a promising renewable resource for production of thermosets. In this project Kraft lignin is sequentially solvent-fractionated and modified in an allylation process with allyl chloride. The allylated lignin is reacted with a cross-linking agent and used to impregnate carbon fibre mats. The resin-coated material is then cured at 125 ºC to achieve a composite material. The project also encompasses characterization of the chemical structure of lignin in the different fractions. The morphology and adhesive properties of the lignin as well as the carbon fibres and the composite material was investigated. Although the production of composite material from lignin and carbon fibres were accomplished, bubble formation in the resin was a problem for all composite samples that were prepared, whether it was during solvent evaporation or during curing. By performing the addition of resin to carbon fibre mats in multiple steps, where pressure is added after the first applied layer, it is suggested that complete adhesion to the carbon fibre can be achieved, whilst maintaining adequate resin to carbon fibre ratio.

Sammanfattning

Marknaden är i stort behov av mer miljövänliga alternativ till fossilbaserade kompositmaterial för att kunna erhålla en mer hållbar framtid. Lignin är den näst vanligaste aromatiska biopolymeren och framställs som en biprodukt i pappersindustrin. Fraktionering av lignin har gjort det möjligt att erhålla lignin med låg dispersitet och molekylvikt vilket är lämpligt för vidare applikationer. Modifiering av lignins struktur ger upphov till nya reaktiva grupper som kan anpassas för ens behov. Den aromatiska strukturen som lignin besitter resulterar i en lovande förnybar resurs för produktion av härdplast. I detta projekt är Kraft lignin sekventiellt fraktionerat med lösningsmedel och modifierat med hjälp av en allyleringsprocess i närvaro av allylklorid. Det allylerade ligninet reagerar med en tvärbindare och används vidare för att impregnera kolfiber. De impregnerade kolfibermattorna härdades i ugn vid 125 ºC för att erhålla kompositmaterial. Projektet omfattar även karaktärisering av den kemiska strukturen i lignin från de olika fraktionerna. Morfologin och vidhäftningsförmåga av lignin, kolfiber och likaså kompositmaterialet undersöktes. Ett kompositmaterial bestående av kolfiber och lignin erhölls med framgång under projektets gång, dock var bubbelbildning ett stort problem under förångningen av lösningsmedel och även under härdningsprocessen. Addition av harts till kolfibermattorna i flera steg, där tryck är adderat efter det första lagret har blivit applicerat, anses vara en lovande metod för att en hög vidhäftningsgrad ska kunna erhållas. Detta medan ett adekvat förhållande mellan harts och kolfiber upprätthålls.

Key-Words: *Kraft lignin*, *Solvent fractionation, Selective allylation, Lignin based composite material, Thiol-ene thermoset*

Table of Content

1. Introduction

In the following section of the report, a short background of the subject will be presented. The aim of the project as well as the scope and method will also be described.

1.1 Background

Thermosetting polymers, also called thermosets, are polymers made by the irreversible crosslinking of monomer units into a network caused by the application of heat or radiation (IUPAC, 1997). Before curing, the monomer solution is often referred to as a resin and is in a viscous liquid form. Most of the thermoset materials used in today's industry is oil-based which includes phenolic and urea formaldehyde resins as well as epoxy resins. Epoxy resins correspond to 70% of the thermosets in the industry, due to their aromatic structure. Aromaticity contributes to desirable properties such as high glass transition temperature (T_g), which implements good strength performance even in high temperatures. Despite the advantages, there are problems with the usage of epoxies. The most common monomers for the synthesis of epoxy is received from the reaction of bis(4hydroxyphenylene)-2,2-propane (bisphenol A, BPA) (Auvergne et al., 2014). The problem is that BPA has significantly harmful effects on both the human health as well as the environment (Frederick and Claude, 2005).

Lignin is the second most abundant aromatic polymer after cellulose on earth and is a renewable raw material, and its structure contains a high degree of phenolic- and carbon content (Aminzadeh et al., 2018). Lignin is an aromatic compound with complex structure which is derived from sinapyl, coniferyl and p-hydroxyphenyl alcohols. There is considerable variety in the ratio between the three alcohols in the structure of lignin, resulting in a large degree of heterogeneity (Simmons, Loqué and Ralph, 2010). Today, lignin is mostly known as a by-product from the pulp and paper industries, where it is burnt to produce energy (Katahira, Elder and Beckham, 2018). However, lignin is a promising resource and may have multiple possibilities appropriate for industrial applications, such as thermosets for adhesives and carbon fibres (Aminzadeh et al., 2018).

To be able to use lignin as a raw material in any application it is of importance to improve the purity and the homogeneity of the biopolymer. The homogenization of lignin can be achieved

through fractionation, where different sized lignin with different molecular weights are separated (Duval et al., 2016). The desired product may then be tailored by choosing the most suitable fraction for the application. Low molecular lignin is suitable for adhesive and carbon fibres applications, while high molecular lignin is more suitable for pyrolysis and fragmentation modification (Jiang et al., 2017).

Further modifications are required to utilize lignin as the main component of a thermoset material, as is done in this project. This is required to achieve a reactive site on the lignin structure. In this project Kraft lignin is fractionated with sequential solvent-fractionation and modified in an allylation process with allyl chloride. To receive a resin capable of thermosetting a cross-linking agent is added to the allylated lignin. The received resin is applied to carbon fibre mats to achieve a composite material. Composite materials are typically made by the combination of a resin matrix and a fibre reinforcement; together the materials combine their individual strengths and make up for their weaknesses. Composites are used in the aerospace, automotive and medical industries to name a few (Rajak et al., 2019).

The project also encompasses characterization of the chemical structure of lignin in the different fractions. Furthermore, the morphology of the lignin as well as the carbon fibres and the composite material is investigated.

1.2 Aim

The intention with this project is to investigate the usage of processed lignin in the production of polymer based thermosets to create a composite material. An assessment of the lignin modification and fractionation, as well as thermosetting of composite will be performed to find the most promising method for creating lignin based composite materials.

1.3 Scope

The focus of this project is to investigate the possibility of lignin applications as composite materials. This is done by assessing the adhesion of the thermosetting lignin resin to carbon fibre mats. Since there are no tensile tests applied to the created material, no conclusions about the material's resistance, nor strength, can be drawn.

1.4 Method Overview

This project is divided in two parts, where the first one is based on research for relevant information and the second one is based on an experimental section.

The first part of this project is based on finding information from literature to obtain knowledge within the specific subject of modifications and applications of lignin. Scientific papers are mainly used where projects in the same area of science have been investigated. The information that is found will further on be applied in the experimental section.

The second part of the project is based on an experimental section where the information that is found will be applied. The experimental section will be divided in two. Phase one of the experimental section consists of the fractionation and modification of the lignin. (The aim is to receive narrow-dispersity lignin, which is suitable for further applications.) This is to receive a narrow dispersity lignin which is suitable for further application. The second phase of the experimental section will concern synthesis of lignin based thermosets, where the lignin thermoset in combination with carbon fibres will be the foundation for the composite material. All of the results are thereafter investigated with multiple analytical methods.

2. Theoretical Background

Lignin is a heterogenous biopolymer that is a byproduct from the pulping industry. The potential of lignin is currently unrealised because of difficulty in handling the lignin. Factors such as raw material and processing methods affect the characteristics of lignin and the potential uses it may have (Laurichesse and Avérous, 2014). The following section describes some of the relevant background information for turning lignin into a composite material.

2.1 Lignin

Lignin is an alkyl-aromatic biopolymer which is also amorphous and heterogeneous (Zhao and Abu-Omar, 2021; Katahira, Elder and Beckham, 2018). It is the main component in cell walls of various plants and it is the second most common biopolymer in nature. The main role of lignin is to stabilize cell walls and give it stiffness. Other important qualities that lignin contributes to is the ability to transport water within the plant as well as provide good protection against insects and microorganisms (Chung and Washburn, 2016). About 15-35% of the plant consists of lignin, depending on the type of plant. Lignin is mainly obtained as a byproduct from the pulping process. The bulk of all produced lignin is burned and used as an energy source in today's industries (Katahira, Elder and Beckham, 2018).

The chemical structure of lignin can vary greatly depending on which plant it is extracted from. This results in a broad variety in the structure and chemical composition of lignin. Lignin consists of three main phenylpropanoid monomers which are *p*-coumaryl alcohol, coniferyl alcohol, and sinapyl alcohol as presented in Figure 1. The major property that varies between these monomers is the number of methoxyl groups connected to the aromatic ring, but the aliphatic chain has the possibility to vary as well. When these three phenylpropanoid monomers are dehydrogenated they become phenoxyl radicals, which are the repeating units in lignin. The three repeating units are *p*-hydroxyphenyl (H), guaiacyl (G) and syringyl (S) which are presented in Figure 2. Different types of plants have different amounts of these building blocks. Lignin in softwood primarily consists of G-units with a small amount of H-units, while lignin in hardwood consists of G-units as well as S-units (Katahira, Elder and Beckham, 2018).

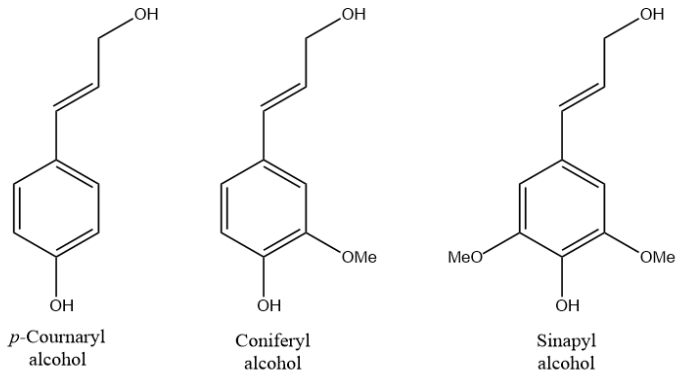

Figure 1: The three main phenylpropanoids monomers.

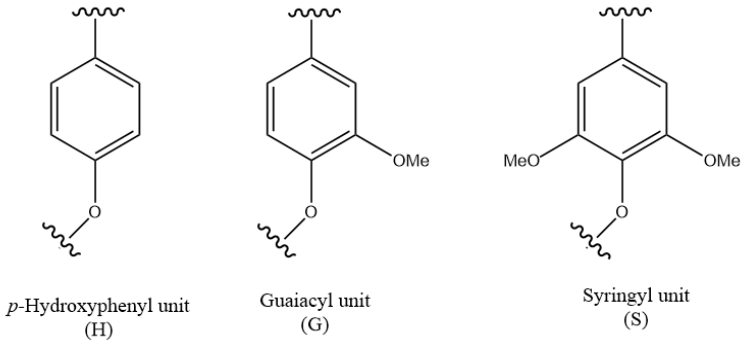

Figure 2: The repeating units of lignin.

Lignin is formed through random polymerisation of the phenoxyl radicals, into a three dimensional structure. The monomers are connected with covalent bonds of different forms, which are randomly positioned in the polymeric chain. However, the primary bond in the polymeric structure is aryl ether bond, β-O-4 (Henriksson et al., 2010). A large variety of functional groups are connected to the building blocks. Some common functional groups are benzyl alcohol, methoxyl, aliphatic hydroxyl, phenolic hydroxyl and carbonyl groups (Katahira, Elder and Beckham, 2018). Depending on the composition of the functional groups the properties of lignin will vary. Properties that can vary are the reactivity, solubility, dispersion characteristics and visual attributes (Huang, Fu and Gan, 2019).

2.2 Lignin as a Resource

Lignin is obtained as a byproduct from the large pulping industry and is currently burnt for heat production. The utilization of lignin in this way is only somewhat better than discarding

it, because of low efficiency. By valorizing lignin and turning it into a resource rather than solely a byproduct, there is hope that lignin will help shift production industries away from fossil based products. The difficulty with lignin however, is its complex and irregular structure, which was described in the previous section. Furthermore, the type of processing method used will also affect the lignin. The lignin used in this project comes from softwood and was obtained from a Kraft pulping process.

There are different processes for obtaining technical lignins such as the soda-, organosolv or Kraft process. Figure 3 shows the general reaction conditions needed for the different methods, although only the Kraft process will be discussed in further detail (Laurichesse and Avérous, 2014).

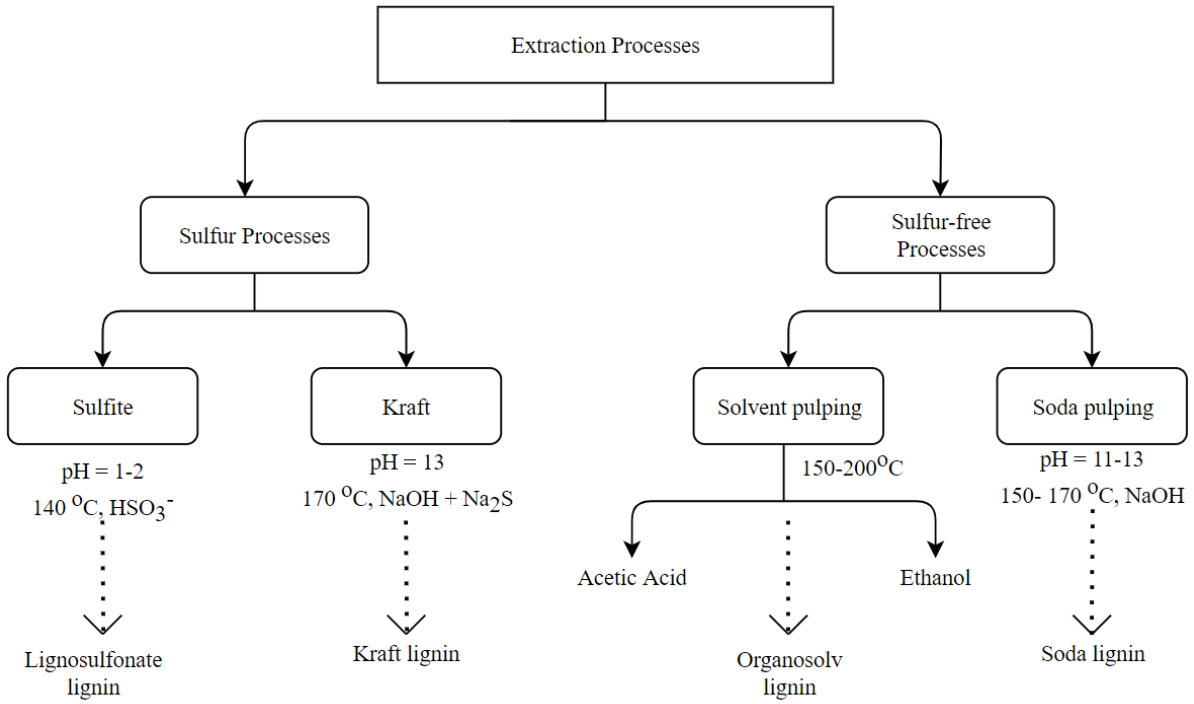

Figure 3. Various processing methods and their necessary operating conditions. The type of extracted lignin will determine the characteristics of the lignin. (Adapted from Laurichesse and Avérous, 2014)

Lignin can vary in properties such as polydispersity, molecular weight and the amount of functional groups, and it is important to understand in which way these factors can affect the processability of lignin (Chung and Washburn, 2016). The Kraft process utilizes sodium hydroxide and sodium sulfide at high temperature and high pH. Through the process ether bonds are broken and a robust lignin complex can be reformed at the end through

condensation reactions. Kraft lignin is hydrophobic at neutral pH and contains roughly the following amounts of functional groups, expressed in weight percentage: 1% aliphatic thiols, 14% methoxy groups, 10% aliphatic hydroxyl groups, 2-5% phenolic hydroxyl groups and 4-7% carboxylic acid groups. (El Mansouri, Farriol and Salvadó, 2006)

Other processing methods used for the production of lignin include hydrothermal, organosolv and dilute acid methods. Hydrothermal methods utilise high pressure and high temperature water to break down lignin. It is currently used to some extent to produce biofuels. The Organosolv and dilute acid methods are still in a laboratory or pilot-scale testing phase. The advantages of these newer methods are that the resulting lignin is of lower dispersity, lower molecular weight, and solvable in a wider range of solvents. However, the organosolv process will probably be quite expensive for the foreseeable future because of the amount of organic solvent needed (Chung and Washburn, 2016).

2.3 Fractionation and Modification of Lignin

The process of turning lignin into more valuable products includes handling the issue of the heterogeneity of lignin and modification to enable further reactions. One of the most common ways of preparing lignin for modification is through solvent fractionation, and it is desirable to choose a good solvent for extracting the sought after components, whilst also keeping green chemistry in mind. Low boiling points to ease solvent recovery and less hazardous solvents are preferable. To modify lignin there are several potential reactions to consider. Allylation with an allyl halide as used in this report, is one of them. This section will go over the methods used for fractionation and modification.

2.3.1 Fractionation of Lignin

Technical Kraft lignins can contribute to the industry of carbon fibres, phenol-based polymers and adhesives. To be able to use lignin as a raw material in chemical products, it is necessary to improve factors such as purity, thermal behavior as well as molecular mass distribution. The heterogeneity as well as the contaminations in lignin are a big limitation for further applications, purification is therefore necessary (Brodin, Sjöholm and Gallerstedt, 2009).

When Kraft lignin is produced in the pulping process it exists in the alkaline pulping liquors also called the black liquors. The Kraft lignin is extracted from the black liquors with a

process called LignoBoost (www.valmet.com, n.d.). This process is required to obtain high quality lignin from the pulping process. The lignin received possess low ash content which is desirable (Tomani, 2010). It is desired to have as pure lignin as possible because of the major effects impurities have on the thermal behavior of lignin. Alterations in the thermal behavior makes it difficult to use lignin for further valuable applications (Sameni et al., 2014). However, the received Kraft lignin still has a relatively high polydispersity. The high heterogeneity of the lignin results in further need of fractionation to achieve the desired dispersity (Duval et al., 2016).

There are multiple types of fractionation methods with different techniques that are promising for fractionation of lignin. Four of these techniques are solvent screening, membrane filtration, sequential precipitation and microwave processing (Duval et al., 2016; Aminzadeh et al., 2018; Jiang et al., 2017; Cederholm et al., 2020).

Solvent screening has been used to find the most appropriate solvents to fractionate Kraft lignin. This has been used to develop strategies in the area which align with the restrictions and requirements within the industry (Duval et al., 2016). Generally a solvent with low boiling point is beneficial due to the energy saving in the later steps of the process when the lignin needs to be separated from the solvent (Katahira, Elder and Beckham, 2018). Furthermore, it is also important to avoid modifications of the lignin during the fractionation. Ethyl acetate, ethanol, methanol and acetone are common industrial solvents that have been shown to work efficiently in the fractionation of lignin. Fractionation is used by implementing the strength of the solvents, i.e. polarity, in increasing order (Duval et al., 2016). The yield and polydispersity of the fraction depends on the chosen solvent. Obtaining fractions with a low polydispersity of around two is desirable; the polydispersity can vary greatly between solvents (Katahira, Elder and Beckham, 2018). Low molecular weight lignin is soluble in all solvents while the ethyl acetate is more selective for the low molecular weight fractions (Duval et al., 2016).

Membrane filtration is a promising technique for receiving high homogeneity of lignin. This technique utilizes ultrafiltration by using ceramic membranes. This method has several advantages but in particular the possibility of extracting the lignin directly from Kraft pulp cooking liquors without adjusting the temperature nor the pH. However, the membranes will

lose efficiency over time which will increase the soiling. An increase of soiling will also make the method less efficient economically (Aminzadeh et al., 2018).

Sequential precipitation is a promising method for franctionating lignin because of the economical and efficiency advantages of the process. The technique involves dissolving the lignin in a solvent mixture which is further on sequentially precipitated. This is implemented by using several different organic solvents which consist of various functional groups. Lignin is in that way fractionated into more homogeneous fractions, which includes lower dispersity and regular molecular mass. The low molecular fraction separated with this method has suitable properties for further application with carbon fibres and adhesive (Jiang et al., 2017).

Microwave processing is another technique that can be used to receive a high yield of narrow-dispersity Kraft lignin. This technique uses a microwave assisted extraction process. The lignin is dissolved in green solvents such as methanol or ethanol while being heated with microwaves. This will separate the soluble fractions from the insoluble fractions of lignin. The aim with this method is to obtain lignin with high yield and narrow dispersion in a faster and more efficient way than other commercial methods. This is a promising technique for future production of lignin based material as it is both green, fast and results in high yields (Cederholm et al., 2020).

Although there are several methods developed for fractionating lignin, every technique has its own advantages and disadvantages. Some disadvantages that can be associated with the methods are low purity and high costs. It is of high importance to develop a fractionating technique that is efficient both economically and in production (Jiang et al., 2017).

2.3.2 Modification of Lignin

In this report solvent fractionated lignin is modified through allylation. Hydroxyl functionalities in the lignin react with allyl chloride to provide the lignin structure with allyl moieties that in turn can react with thiol cross-linkers to produce a rigid thermoset material (Jawerth et al., 2017). Figure 4 shows a schematic overview of the process.

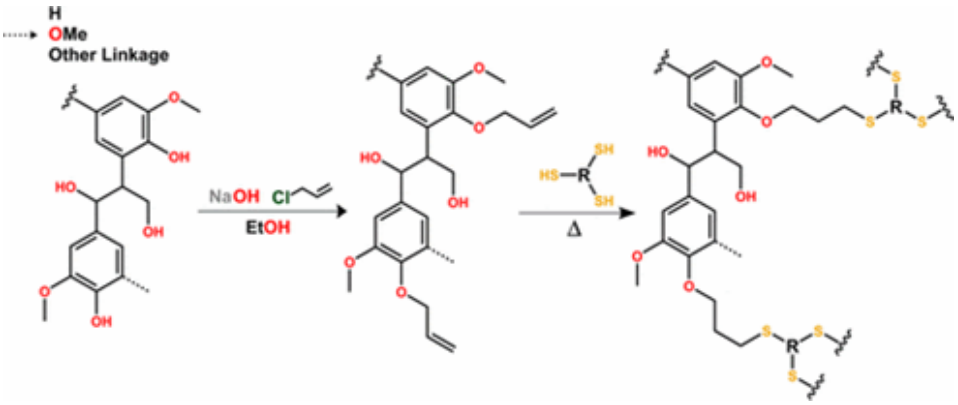

Figure 4. General overview of the allylation pathway. (Image source: Jawerth et al., 2017)

The allylation reaction is highly selective and has proven to specifically target phenolic hydroxyl groups in the presence of aliphatic and carboxylic hydroxyls. Allylation occurs through a base-catalyzed Sn2 reaction where the deprotonated hydroxyl group attacks the halogen-attached carbon. Chloride is a good leaving group which facilitates the reaction, and the solvent choice of ethanol and basic conditions works well to both solve the allyl chloride and lignin (Jawerth et al., 2017). Allyl bromide is also a viable option for allylation reactions, and is more reactive. It is also less selective than allyl chloride and reacts with aliphatic hydroxyl content to a larger extent (Luca Zoia et al. 2014).

The process is green since ethanol is a readily available green solvent, and the reaction temperature of 65 ℃, which is to be maintained for 40 hours, is well within reason when keeping in mind the potential benefit of replacing fossil-based materials. Allyl chloride, however, is highly toxic and has long lasting negative effects on aquatic environments. Furthermore, it is produced through chlorination of propylene, which mainly comes from fossil sources (Mohammad Armanmehr, Fatemeh Mohajer and Elham Khademloo, 2013).

A commercially existing process for utilizing lignin is in the production of the important solvent dimethyl sulfoxide (DMSO). The lignin is dealkalized, meaning that methyl groups are removed from the lignin. The process involves molten sulfur in alkaline media and the abstracted methyl groups react with the sulphur to produce dimethyl sulfide (DMS), which is then further oxidized with nitrogen dioxide to produce DMSO (Laurichesse and Avérous, 2014). There is also alkylation of lignin, which is the process in which alkyl groups are added onto lignin molecules. Alkylated Kraft lignin has demonstrated the ability to form brittle

polymeric materials that can be plasticized by addition of aliphatic polyesters (Li and Sarkanen, 2002).

There are many other ways to modify lignin in addition to those mentioned, and they all provide interesting pathways to make use of lignin as a raw material. Oxypropylation, epoxidation, acetylation and silylation are a few examples (Laurichesse and Avérous, 2014; Gioia et al., 2018; Buono et al., 2016). Oxypropylation is an etherification reaction that utilizes alkylene oxide, most commonly propylene oxide, to form new ether bonds. Like allylation, the reaction is selective towards phenolic hydroxyls, and could be used to make epoxy resins and polyurethane. However, it reacts slower with Kraft lignin in comparison to organosolv lignin, which is not as available commercially (Laurichesse and Avérous, 2014).

Epoxidation is another possible pathway, and one such example is the one studied by Gioia et al. where phenolic hydroxyls are converted to oxirane moieties and reacted with an aliphatic diamine to produce a thermoset material. The results were promising since the final material could be produced with tuneable thermo-mechanical properties, with controllable factors such as molecular weight (Gioia et al., 2018). In comparison to the previously mentioned methods, acetylation and silylation are pathways that modify all the hydroxyl content of lignin. Some 15% of aliphatic hydroxyls are left unreacted due to steric hindrance, and potential uses may be as an antioxidant additive for polyolefins. The silylated lignin is of particular interest because of its high thermal stability, in comparison to acetylated lignin, and wide range of solubility in organic solvents (Buono et al., 2016).

Another interesting modification of lignin is the two-step process as described by Luca Zoia et al. (2014), where lignin is allylated with allyl bromide and then heated in the presence of dimethylformamide (DMF). The allylated lignin undergoes a Claisen rearrangement that frees up hydroxyl functionalities where there once was an ether bond. The reaction is a pericyclic reaction of [3,3]-sigmatropic rearrangement (Clayden, Greeves and Warren, 2012, pp.909–910), and Figure 5 shows the reaction. The freed-up hydroxyl groups could undergo further modification, or provide the lignin with antioxidizing properties. (Luca Zoia et al., 2014)

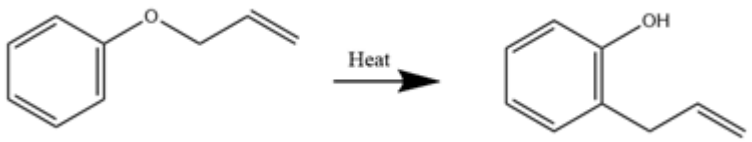

Figure 5. Claisen rearrangement reaction.

2.4 Composite Materials

Composite materials are a combination of a matrix and reinforcement nested within the matrix, this combination of two materials with different characteristics offers the synergistic benefits of both materials while minimizing the downsides of the individual components. Common matrix materials include polymers, ceramics and metals (Sharma et al., 2020). Choice of reinforcement material is dependent on the employed matrix, for polymer matrices common reinforcement materials include carbon, glass, kevlar and metal fibres (Rajak et al., 2019). Composites are used in many various applications due to their high strength to weight ratio along with other more specialized, tunable characteristics (Rajak et al., 2019; Sharma et al., 2020).

2.4.1 Thermosets and cross-linker Reactions

As described in the background section, thermosets are polymers created by the irreversible crosslinking of monomers into a network caused by the application of heat or radiation (IUPAC, 1997). Before curing, the monomer solution is often referred to as a resin and is in a viscous liquid form. Thermosets often have the characteristics of being rigid, chemically resistant and impact resistant though the exact properties of a thermoset depend greatly on the chemistry of said thermoset (Bpf.co.uk, 2021; Shokuhfar and Arab, 2013). The majority of thermoset use can be attributed to polyesters, phoplasts, epoxy resins, polyurethanes and polyimides (Hsissou et al., 2021).

In order for the monomer units to join together in a network and form a thermoset a cross-linker molecule is often used to bind together multiple monomer units. In the case of epoxy resins the most commonly used system is composed of bisphenol A diglycidyl ether (DGEBA) and a polyamine which is the cross-linker or curing agent (Liquid Epoxy Resins

DOW, n.d.). A selection of representative polyamine cross-linkers used for curing epoxy resins are presented in Figure 6 (Liquid Epoxy Resins DOW, n.d.;Wan et al., 2012).

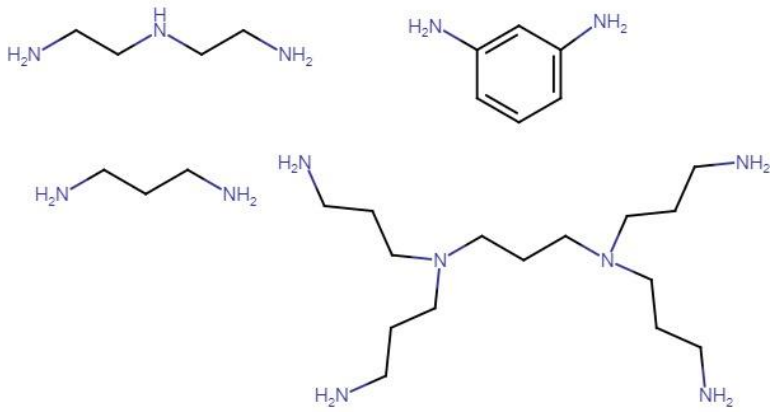

Figure 6. A selection of polyamine cross-linkers used in the curing of epoxy resins.

The epoxy-amine system utilizes the bond forming reaction between epoxide groups and amine groups to form an interconnected polymer network. The epoxide-polyamine system described above is only one of many thermosetting systems.

In this study thiol-ene chemistry is used in order to construct lignin based thermosets. The thiol-ene platform was first described in 1905 by Theodor Posner and is characterised by high yield reactions, versatility in reactants, little to no side products, insensitivity to oxygen and fast reaction rates (Hoyle and Bowman, 2010). There are numerous mechanisms for thiol-ene reactions, however the free radical reaction mechanism is one of the more practical and well studied reactions and is known for its efficiency and step-growth nature (Hoyle and Bowman, 2010). In this study allylated lignin is reacted with the trithiol cross-linker Trimethylolpropane tris(3-mercaptopropionate) (3TMP) presented in Figure 7.

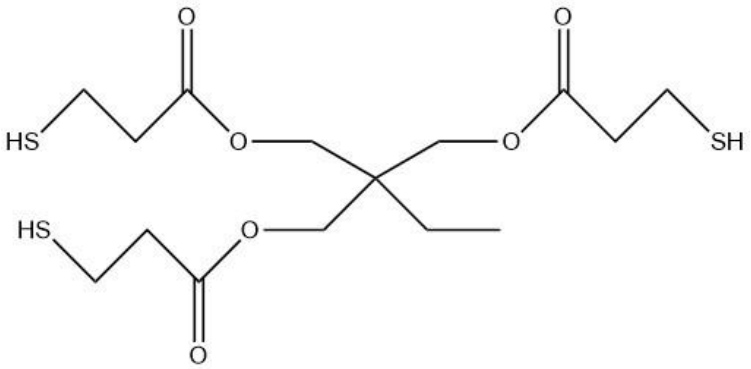

Figure 7. Structure of 3TMP.

Allyl groups attatched onto the lignin are reactive towards thiol groups and form the polymer network upon heating. Figure 4 shows the general modification and crosslinking procedure and products while Figure 8 presents a more detailed mechanism for crosslinking including initiation, propagation and termination (Hoyle, Lee and Roper, 2004). Termination of the secondary carbon radical can occur in a number of ways as described by Hoyle, Lee and Roper. One possibility is that the radical reacts with an unreacted thiol from 3TMP and abstracts its hydrogen and transfers the radical onto the cross-linker thiol. Another way the carbon radical can theoretically terminate is by reacting with another carbon radical and making a covalent bond, alternatively the radical could react with an allyl group and propagate in such a way. A thiol radical can also terminate by reacting with another thiol radical and thereby creating a disulfide bond (Hoyle, Lee and Roper, 2004; Koo et al., 2010).

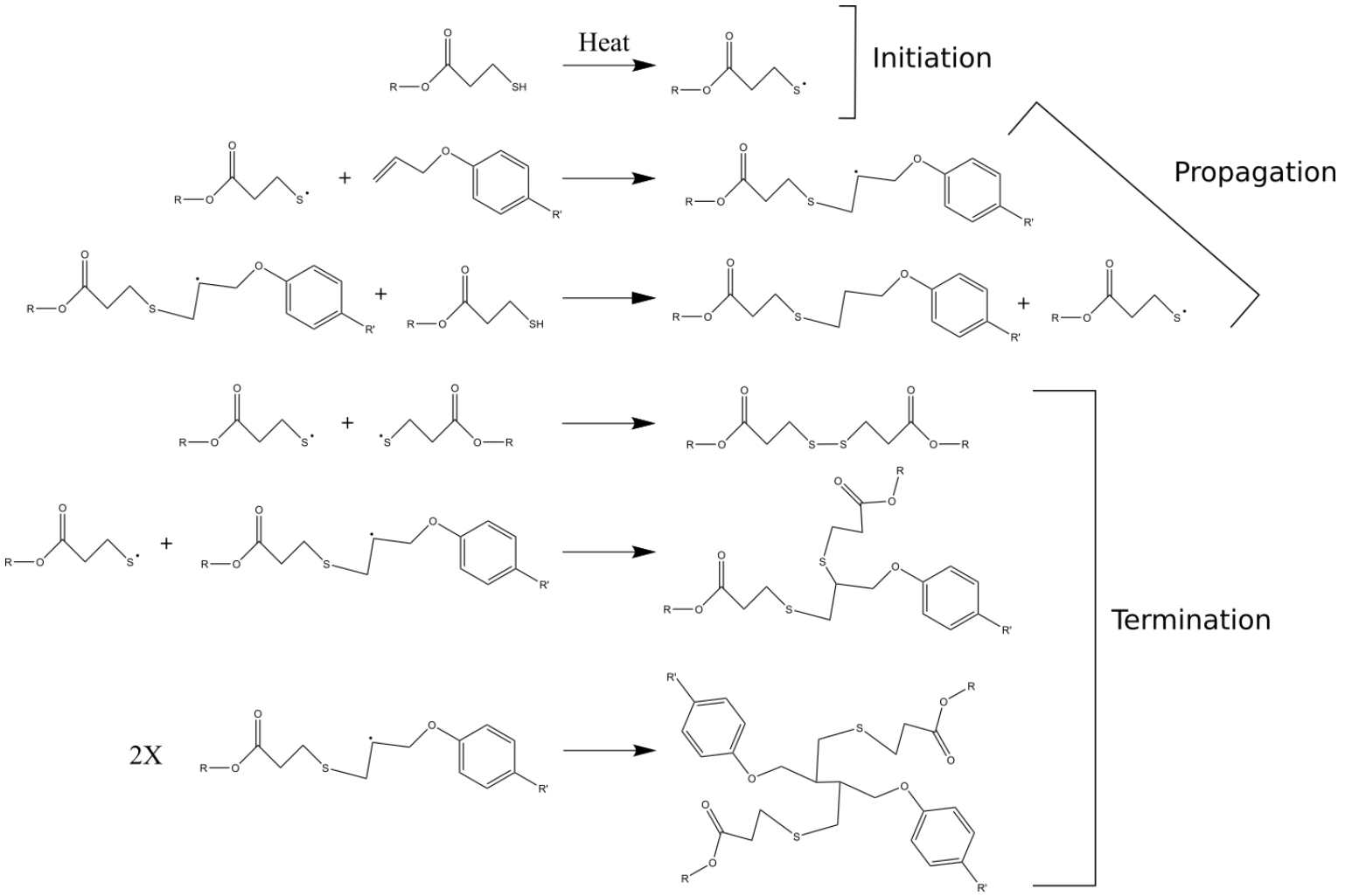

Figure 8. Radical initiation of 3TMP, propagation and termination mechanism with allylated lignin.

2.4.2 Interfacial Adhesion and Matrix Cohesion Properties of Composites

Composite strength is a function of partially the strength of the matrix, the reinforcement and the connection between the two phases. In order to achieve a good adhesion between matrix and reinforcement it is important that both elements share the same general chemical characteristics such as hydrophilicity/hydrophobicity (Jawaid, Thariq and Naheed Saba, 2019). When put under stress composite materials can break in two primary ways, these are adhesive failure and cohesive failure.

Adhesive failure is dependent on poor binding of the matrix to the reinforcement material. Adhesive failure is apparent due to the fracture in the composite upon breaking occuring on the surface of the reinforcement material, represented by the red dashed circle in Figure 9. Assuming poor interfacial adhesion whole fibres of reinforcement material will be pulled out from the composite without much or any resin coating them (Ramezani Kakroodi, Kazemi and Rodrigue, 2013).

Strong interfacial adhesion is apparent when the matrix and reinforcement materials do not slide apart under stress but rather stay together and act as one homogenous solid. Instead of fibres being pulled out from the matrix under stress they will snap due to good interfacial adhesion. By definition good adhesion will be also evident by observing fibres coated with resin in a cross section of a broken composite. When interfacial adhesion is good, fractures in the composite tend to happen in the bulk matrix as shown by the green dashed line in figure 9 (Ramezani Kakroodi, Kazemi and Rodrigue, 2013).

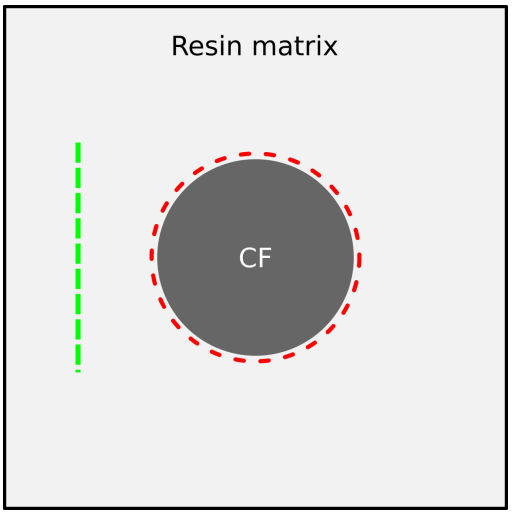

Figure 9. Cross section of composite

2.4.3 Composite Preparation Procedures

Commercially there are many methods used to produce polymer composite materials, here a selection of common methods are presented.

A common infusion method that is widely used today is vacuum infusion. In this process reinforcement material is placed into a mold and a plastic film is placed over the mold and secured so that it is airtight. A vacuum is pulled in the mold assembly and the reinforcement material is firmly compressed into the contours of the mold, low viscosity resin is then allowed to stream in through valves attached to one or more places on the mold assembly. The reinforcement material is infused with resin which is pulled through the mold due to the vacuum. Once infusion is complete the assembly can be transferred to an oven should additional heat be necessary for curing (McIlhagger, Archer and McIlhagger, 2015).

Compression molding is a method for composite production consisting of two phases, first a resin and reinforcement plate is made where resin is distributed onto a plate followed by a layer of reinforcement material and once again a layer of resin. The resin is allowed to gel and increase in viscosity until it can be easily handled. The preformed composite sheet is cut to size and inserted into a hot compression mold where the viscosity of the resin decreases, allowing it to penetrate into the fibre reinforcement and then cure due to the applied heat; the finished part is finally demolded (Park and Lee, 2012).

Pultrusion is a continuous method used for creating profile elements of various designs. The process builds upon the continuous pulling of reinforcement fibres through a vat of resin followed by forming guides and further to a heated die where the designed profile assumes its final form and cures. The part is pulled into a cooling region and a post processing region where it is cut to size (McIlhagger, Archer and McIlhagger, 2015).

3. Experimental

The experimental section describes the methods, amounts and types of chemicals, and software settings that were used in this project. The method section is divided into two parts, where the first part describes the laboratory procedures used to prepare the samples, and the second part describes the analytical methods.

3.1 Materials

LignoBoost softwood Kraft lignin from Stora Enso was used. Ethanol (EtOH, ≥96%) methanol (MeOH, ≥ 99.8%), acetone (≥99.5%) and hydrochloric acid (HCl, 37%) were ordered from VWR. Sodium hydroxide (NaOH,≥98%), chloroform D ($CDCl_3$, ≥98%), 2-Chloro-4,4,5,5-tetramethyl-1,3,2-dioxaphospholane (TMDP, ≥95%), trimethylolpropane-tris(3-mercaptopropionate) (3TMP, ≥95%) and allyl chloride (98%) were ordered from Sigma-Aldrich. All other chemicals used were of analytical grade and ordered from Sigma-Aldrich

3.2 Preparation and Synthesis Methods

The washing and solvent fractionation process builds upon work done by Duval et al., 2016. The modification and thermosetting processes are adapted from work done by Jawerth et al., 2017. The method provides a promising route to produce thermoset materials for use in composite materials. The following section describes the method used in detail, for each of the steps. Figure 10 shows a general outline of the steps conducted in this report in order to prepare all the samples and the modified lignin.

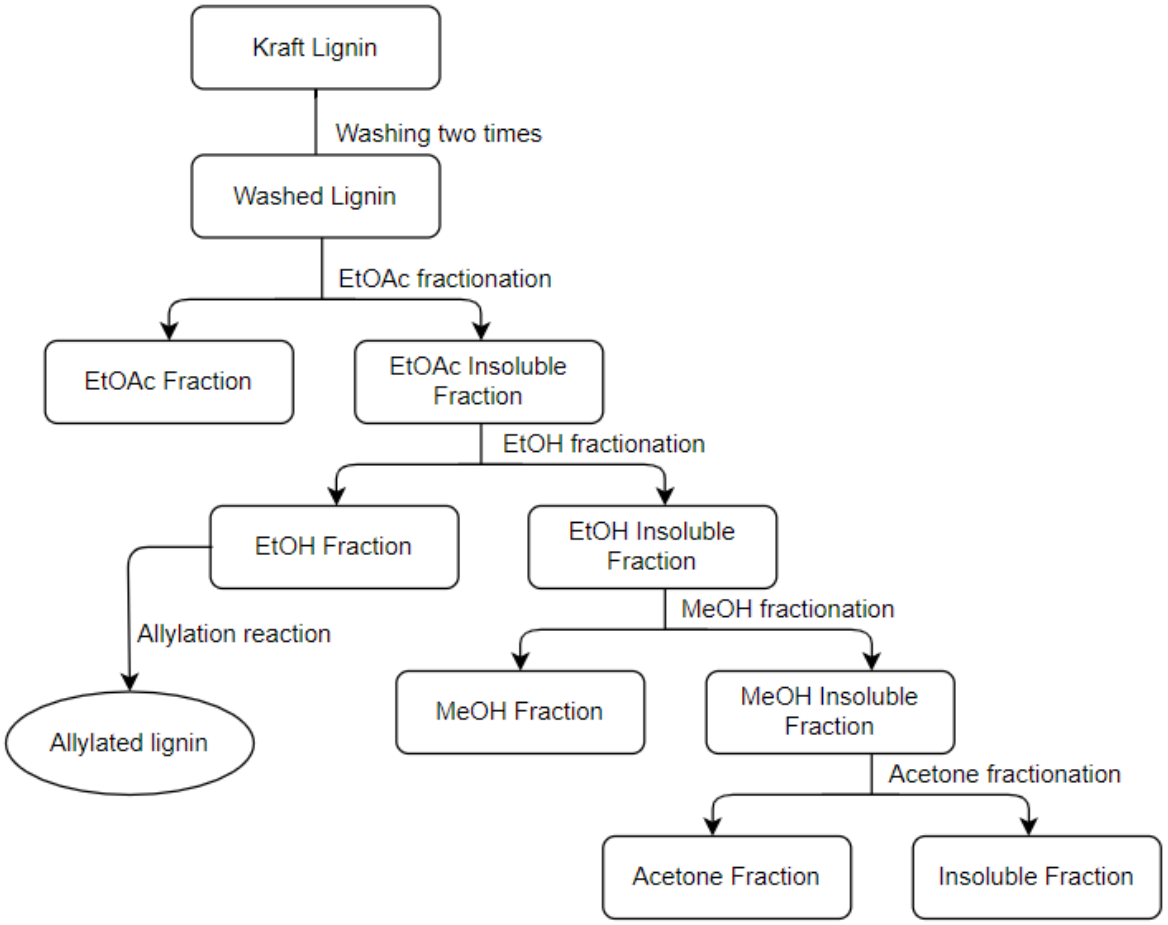

Figure 10. Flowchart describing the steps in the experimental procedure.

3.2.1 Washing

In order to reduce impurities such as ash content and acids from the production process, the lignin was washed. Seventeen batches of 20 g Kraft lignin each were washed in 200 ml of deionized water at 60 ℃ for one and a half hours at a time with magnetic stirring applied. After each round of washing the lignin was filtered off by vacuum filtration through a sintered glass disc and the pH of the washing liquid was tested. This washing step was carried out two times for each batch of Kraft lignin, the pH of the used washing water was checked and all batches satisfied the condition of pH 5.5. If the pH of the water was under 5.5 the washing process was repeated in the same manner as previously described. If the pH value of the water exceeded 5.5 the washing was concluded. After washing the lignin was vacuum dried for approximately 17 hours at 50 ℃.

3.2.2 Solvent Fractionation

From each batch, 15 g of washed Kraft lignin underwent solvent fractionation with ethyl acetate, ethanol, methanol and acetone respectively, in that order. The following procedure was used for all the solvent fractionation steps. The weighed-out lignin was placed into a beaker together with 150 mL of solvent and stirred vigorously by a magnetic stirrer for 2 hours. The dispersion was vacuum filtered through a Munkell grade 3 filter paper, and the resulting soluble fraction was transferred to a small round bottom flask while the insoluble fraction was placed in a beaker. The beaker containing the insoluble fraction was dried in a vacuum oven for 20 hours. After drying the insoluble fraction was processed again with another solvent as described above. The soluble fraction was recovered by using a rotary evaporator, then redissolved in about 15 mL of acetone and precipitated in 200 mL of deionized water. Finally, the soluble fraction was freeze dried to obtain a fine powder.

3.2.3 Selective Allylation Reaction

Only the ethanol fraction from each batch was allylated, targeting the phenolic hydroxyl groups by performing the reaction with an excess of NaOH and allyl chloride. Approximately 1.4 mmol per 1 mmol of phenolic hydroxyl functionalities was used, determined by Phosphorus-31 Nuclear magnetic resonance (^{31}P-NMR). The ethanol fraction of lignin contained approximately 4.6 mmol OH-groups per gram of lignin, see results. This results in ~6.5 mmol of allyl chloride and NaOH needed per gram of lignin.

For each batch prepared, 2 g of lignin was added to a two-necked round bottom flask containing 110 mL of an EtOH/NaOH solution of a 60:40 ratio. The allyl chloride is soluble in ethanol, whilst the high pH caused by NaOH increases the solubility of Kraft lignin by facilitating the deprotonation of the phenolic hydroxyls. The round bottom flask was equipped with a condenser, immersed in an oil bath, and heated to 65ºC. Through careful pipetting the allyl chloride was added dropwise and the reaction was left to run for 40 hours.

The reaction was then stopped and the round bottom flask left to cool off. Once the reaction mixture was around room temperature it was precipitated by adding 0.1 M HCl dropwise until the pH had reached below 4. Subsequently the mixture was filtered through Munktell grade 3 filter paper and washed with 400 mL of deionized water. The filtrate was dissolved using 1-2 mL of acetone and precipitated in deionized water to obtain a homogenous water dispersion. Finally, the dispersion was freeze-dried to obtain a fine brown powder.

3.2.4 Thermosetting of Resin

The lignin resin was prepared by mixing 3TMP with allylated lignin at 1:1 ratio. The amount of 3TMP required for each batch was determined through ^{31}P-NMR, and the amount of lignin was kept at two times the weight of the carbon fibre mat (CF) that was to be impregnated. Some other CF to lignin ratios were used as well, but ended up discarded because of poor results.

A combination of acetone and ethanol was used as a cosolvent for the resin, and different ratios of (ethanol:acetone) 1:1, 1:2 and 0:1 were tested. Acetone evaporates faster, and resulted in bubble formation in the resin. Bubbles introduce weak points in the matrix and are not desirable for the type of composite material that this project aims to produce. To slow evaporation ethanol was used, with varying degrees of success in solving the bubble problem. A 1:2 - ethanol:acetone ratio yielded the most consistent results, and were used for the majority of samples. However, even though less bubble formation was seen during preparation, bubbles would still arise during the curing step.

To cure the resin an initial temperature of 50 ºC was used, mostly for evaporating any residual solvents. Then, stepwise, the temperature was increased to 75, 100 and 125 ºC, totalling in about 20 hours of curing above 100 ºC. Some samples were pressed down during curing, to see if pressure would have an effect on adhesion to the CF, or bubble formation in the resin.

3.3 Analytical Methods

The following section describes the analytical methods, and any relevant preparation steps for performing the type of analysis in question.

3.3.1 Size Exclusion Chromatography

Size exclusion chromatography (SEC) was performed with a SECcurity 1260 infinity GPC system (Polymer Standards Service, Germany) and was used to determine the molecular weight distribution and polydispersity of the lignin samples. The equipment in the instrument that was used was a refractive index with ultraviolet light at 280 nm. The columns were a PSS GRAM precolumn and two PSS GRAM separation columns with a particle size of 100

to 10000 Å. The columns were kept at a temperature of 60 ºC and the eluent used was DMSO solution with lithium bromide (LiBr) in a 0.5% w/w ratio. The solution was flowing at a rate of 0.5 mL per minute. The samples were prepared by being dissolved in a DMSO/LiBr solution with a concentration of 5 mg/mL. The solution was filtered through a syringe filter with a pore size of 0.45 µm. The molecular weight range was set to 342-708000 DA for standard calibration.

3.3.2 Phosphorus-31 Nuclear Magnetic Resonance

^{31}P-NMR was performed to measure the content of hydroxyl groups in the different fractions of lignin. There are three types of hydroxyl functionalities in lignin, namely aliphatic, phenolic, and carboxylic, and each is possible to quantify through this method of ^{31}P-NMR analysis. To perform the analysis the hydroxyl functionalities in lignin are phosphitylated and subsequently quantified through ^{31}P-NMR spectroscopy. The method was developed from the work of Meng et al. (Meng et al., 2019) which builds upon and summarizes recent developments in biomass characterization methods. Some parts have been adapted in accordance with Ribca's recent work (Ribca et al., 2021)

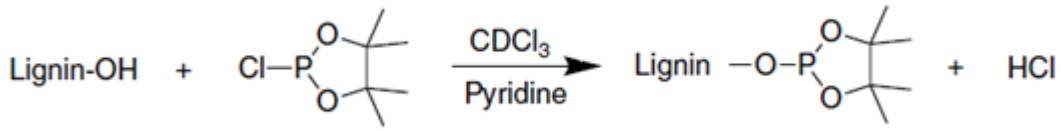

Figure 11. Schematic view of the phosphitylation reaction that enables ^{31}P-NMR analysis of lignin. (Source: Figure has been adapted from Meng et. al, 2019)

The procedure of ^{31}P-NMR was accomplished through several steps, where the first step was to prepare an internal standard (IS). The desired total volume of the IS was 500 µl which is sufficient for approximately nine samples. Endo-N-hydroxy-5-norbornene- 2,3-dicarboxylic acid imide (eHNDI, 97%) was weighted to 30 ± 0.5 mg and added to a vial. Chromium (III) acetyl acetonate was used as a relaxing agent, and 2.5 ± 0.5 mg was added to the IS mixture. The IS, eHNDI and relaxing agent were dissolved thoroughly in 500 µl of anhydrous pyridine (99%), and the solution got a purple colour. Once the IS is prepared and added to the sample it will remain stable for up to four hours before degradation of the IS begins (Stücker et al., 2018).

The lignin sample was prepared by first adding an amount of 30 ± 0.5 mg lignin to a vial. The lignin was thoroughly dissolved in 100 µl pyridine and 100 µl N,N-dimethylformamide (DMF, 99.8%). When the lignin had dissolved, 50 µl of the IS solution was added to the sample and stirred. The derivatization agent (i.e. the phosphitylating reagent) was added to the solution, which in this case was 2-chloro-4,4,5,5-tetrametyl-1,3,2-dioxaphospholane (TMDP, 95%). An exothermic reaction occurred in this step, resulting in the formation of a precipitate. To dissolve the precipitate, 400 µl deuterated chloroform ($CDCl_3$) was added. The final solution was placed in an NMR tube, and then let to rest for approximately 20 minutes to enable complete phosphitylation before ^{31}P-NMR analysis.

^{31}P-NMR was done using a Bruker Avance III HD 400 MHz instrument with a BBFO probe equipped with a Z-gradient coil. 128 scans with a relaxation delay of 10 seconds were used. The total analysis time of each sample was approximately 25 minutes. MestreNova was used for analysing the spectra, and each spectrum was processed in the same way to ensure consistent data handling. A phase correction and a baseline correction was performed, where the settings were set to ’Bernstein Polynomial Fit’ of degree 3.

Three strong signals were expressed in the spectrum, see Appendix A. The first peak from the right corresponds to TMDP reacted with water and was shifted to 132.2 ppm. There it functions as a reference point for all other integrals. The second high peak, representing the internal standard, was integrated between 152.20-151.55 ppm and set to equal 1. The third peak was any remaining derivatization agent, and its presence indicates that the phosphytilation reaction had gone to completion. Three integration areas for the different hydroxyl groups were then entered accordingly: aliphatic hydroxyl groups between 149.50-145.50 ppm, phenolic hydroxyl groups between 144.70-137.00 ppm, and the carboxylic hydroxyl groups were integrated between 136.00-133.60 ppm. The values of the integrals were calculated into mmol per gram of lignin for further experiments and yield.

3.3.3 Proton Nuclear Magnetic Resonance

Proton nuclear magnetic resonance (^{1}H-NMR) was used to identify allyl functionalities in the modified lignin. Ethanol soluble fractions of lignin were weighed to 25 ± 0.1 mg and placed in a vial. The lignin was dissolved in 550 µL DMSO-d6, and the solvent signal at 2.50 ppm could be used as an internal reference signal for chemical shifts (δ). The spectra were

recorded with a relaxation delay of 5 s, a number of scans of 128, and an acquisition time of 4.9 min.

3.3.4 Thermogravimetric Analysis

To study the thermal stability of the lignin soluble samples a thermogravimetric analysis (TGA) was done with a Mettler Toledo TGA/DSC1 instrument. 10.2 ± 0.3 mg of the lignin samples were placed in the machine. The samples were kept at 30 ^{o}C for 10 minutes and then heated to 800 ^{o}C with a rate of 5 ^{o}C per minute and then maintained at that temperature for 10 more minutes. The Mettler-Toledo STARe software V15.00a was used to record the data.

3.3.5 Differential Scanning Calorimetry

Two samples of each fraction, as well as Kraft lignin, and allylated lignin were analysed with differential scanning calorimetry (DSC). The samples were placed in aluminium crucibles and analyzed with Mettler Toledo DSC1 equipped with a sample robot. Inert nitrogen gas was passed through the cell at a rate of 50 mL per minute in order to avoid any reactions with oxygen during heating. The weight of the samples were 10.2 ± 0.6 mg and the crucibles were fitted with punctured lids. The type of DSC used was the Heat-Flux variant, where both reference and sample are placed in the same cell, and the temperatures of the sample and reference follow a predetermined programme. All rates of heating and cooling were set at 10 ^{o}C per minute.

All the samples underwent two cycles of heating. The first cycle had the purpose of removing any thermal history from the sample, since long time storage, or sudden cooling/heating can alter the properties of the sample. This was done by heating the sample to 105 ^{o}C and maintaining it there for 20 minutes. Afterward the sample was cooled to 20 ^{o}C again and maintained there for 10 minutes. The second cycle is the actual testing and the sample was heated to 300 ^{o}C. Such a high temperature is above lignin's degradation temperature, which has been assessed through TGA.

3.3.6 Fourier-Transform Infrared Spectroscopy

Qualitative chemical analysis was carried out by use of attenuated total reflectance fourier-transform infrared spectroscopy (ATR FTIR) with a PerkinElmer Spectrum 100 spectrometer. All samples were analyzed through the Golden Gate ATR element equipped

with a diamond crystal and the spectra obtained by averaging 16 scans. The resulting spectra were compared to each other to monitor chemical changes throughout the whole laboratory process. One specific signal that was expected to be identified with this method was the allyl group signal after the allylation reaction.

3.3.7 Scanning Electron Microscopy

Samples for analysis by scanning electron microscopy (SEM) were thoroughly dried and fastened to a height adjusted metal stage with carbon tape. Excess lignin was removed by blowing with compressed air in the case of lignin morphology analysis. All samples were sputter coated with platinum/palladium to increase conductivity, the signal to noise ratio and to reduce sample drifting/charging. The sputter coater used was a Cressington Sputter Coater 208 HR.

Coated samples were subsequently analyzed with a Hitachi S-4800 scanning electron microscope. Lignin samples were analyzed with a voltage of 1 kV, resin carbon fibre composites at 5 kV and bare carbon fibres at 5kV.

4. Results and Discussion

The results from the experimental section will be presented and analysed in the following section. The purification and fractionation as well as the allylation and the final composite material will be analysed and discussed based on the results from the analytical techniques. The result will be presented in the course of the events, which means that the purification and fractionation will be presented first, followed by the allylation and lastly the final composite material.

4.1 Purification and Fractionation

The results of purification and fractionation of Kraft lignin will be summarized and discussed in this section. Focus will be on describing how the process has affected the characteristics and morphology of the fractions.

4.1.1 Purification

The Kraft lignin was washed twice to remove salts, ash content, and any other impurities. The washed lignin was analysed with SEC, TGA, DSC, FTIR and ^{31}P-NMR. It was concluded that the washing step had little to no effect on the lignin and the washed lignin is very similar to the initial Kraft lignin. Appendix B, C and D contains SEC, FTIR and ^{31}P-NMR graphs for reference. Ash content analysis would confirm that the washing step decreases the amount of unwanted impurities in the samples, and this has been reported in earlier works (Ribca, 2021)

4.1.2 Sequential Fractionation

The washed lignin was sequentially solvent-fractionated into four fractions, plus the insoluble fraction, in order to achieve better homogeneity and lower dispersity. The fractions were analysed with SEC, TGA, DSC, FTIR and NMR. Table 1 shows results from SEC analysis and includes the yield, number average molecular weight (M_n), weight average molecular weight (M_w) and dispersity (Đ). At least three sets of data were collected and averaged for each fraction, which were sampled from different batches. For all the solvent-fractionated samples the M_w and dispersity is lower when compared to the initial lignin and the insoluble fraction.

During fractionation the solvent strength, i.e. the polarity, within the series was used in an increasing order, which means that ethyl acetate was used for the first fractionation followed by ethanol, methanol and lastly acetone. The correlation between molar mass and solubility is evident, as for example can be seen when looking at the EtOAc fraction, which has a remarkably lower molecular weight than the acetone fraction, comparing 900 Da and 3500 Da. The insoluble fraction had by far the largest molecular weight, with a value of 19300 Da, which explains the difficulties in solving this fraction. The trend in M_w is that it increases for each step in the fractionation process, whilst the dispersity is about the same. The yield is best for the EtOAc and EtOH fractions. Figure 12 shows the plotted data from SEC analysis.

Table 1: SEC Results and Fractionation Yields

	Yield [%]	**M_n [g/mol]**	**M_w [g/mol]**	**Đ**
Kraft Lignin (KL)	-	1900	6150	3.2
Washed	-	1950	6700	3.4
EtOAc	20	650	900	1.4
EtOH	18	1200	1800	1.5
MeOH	9	1700	2500	1.5
Acetone	11	2300	3500	1.5
Insoluble	43	6100	19300	3.2
Allylated EtOH	-	1150	1950	1.7

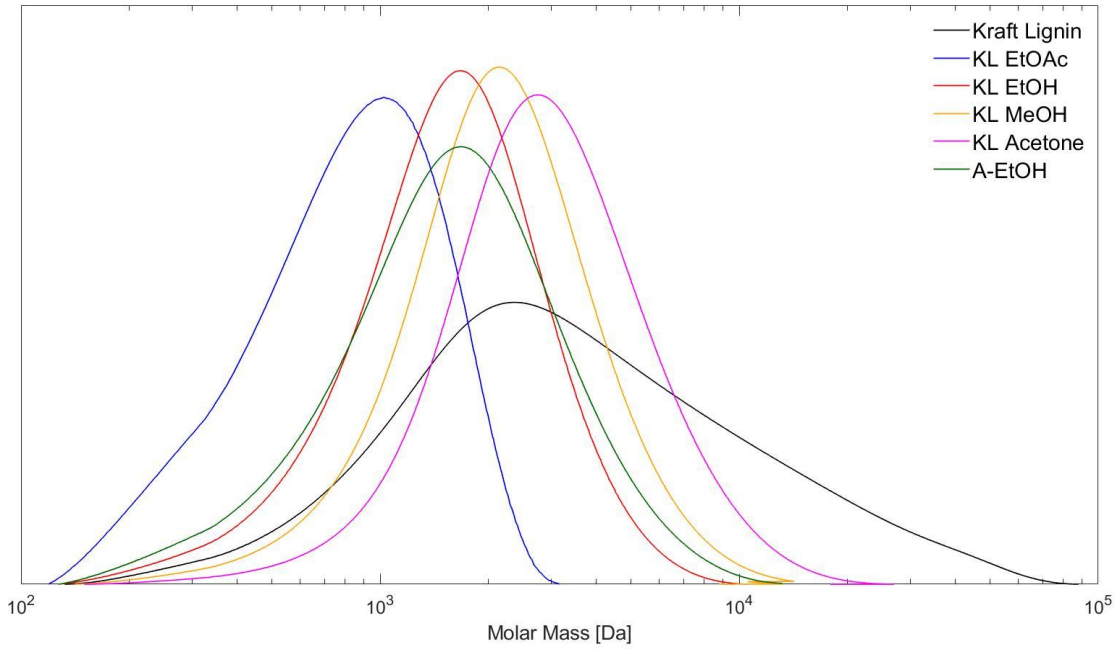

Figure 12. SEC results of the Kraft and solvent-fractionated lignin, as well as the allylated fraction.

4.1.3 Hydroxyl Content

The abundance of hydroxyl content is important for any further modifications, as it is the reactive site that is targeted in the allylation reaction. It was quantified through ^{31}P-NMR and the amount of aliphatic, phenolic, and carboxylic hydroxyl functionalities were calculated from the spectra containing an added internal standard. Figure 13 shows the spectra of all fractions and which regions contain which type of hydroxyl functionality. Table 2 contains the amount of hydroxyl functional groups in mmol/gram of lignin.

For each step of fractionation from EtOAc to Insoluble there is a trend of increasing aliphatic functionality. For the phenolic and carboxylic functionalities, the trend is the opposite, where the relative amounts decrease as the fractionation process is continued. Although a high yield of phenolic functionality is sought after, as can be found in the EtOAc fraction, there are other factors that influence the choice of which lignin to process further. These include molecular weight, solubility, and yield.

Table 2. Hydroxyl functionality content in all fractions

	-OH functionality [mmol/g lignin]		
	Aliphatic	**Phenolic**	**Carboxylic**
Kraft Lignin	2.39	3.83	0.45
Washed	2.50	4.04	0.43
EtOAc	1.14	5.82	0.81
EtOH	2.17	4.29	0.51
MeOH	2.44	4.21	0.38
Acetone	2.11	4.2	0.37
Insoluble	2.89	3.09	0.29
Allylated	1.89	0.61	0.47

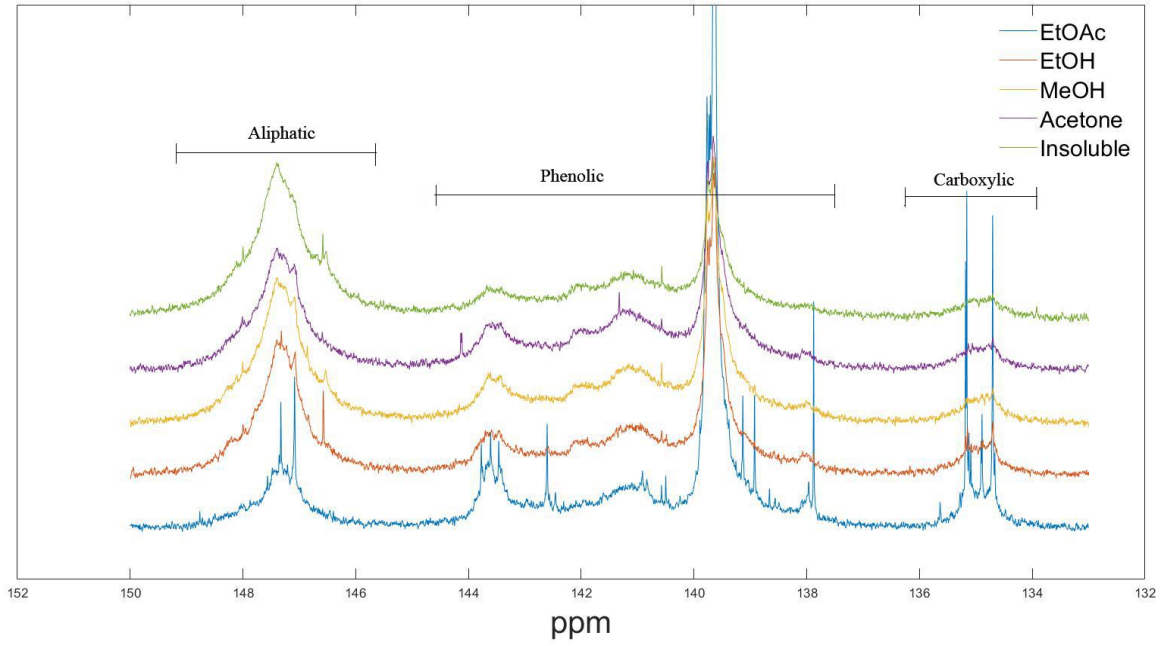

Figure 13. ^{31}P-NMR of all fractions.

A factor that can interfere with ^{31}P-NMR measurements is the stability of the internal standard, so to minimize any effects of IS degradation the sample was prepared and analysed within 2 hours. The IS degrades gradually, and after about 4 hours the -OH content in the sample will be measured as 5-10% larger, and after 10 hours about 10-20% larger, due to IS degradation losses (Ribca, 2021).

4.1.4 Thermal Analysis

Thermal stability and T_g of all fractions were assessed from TGA and DSC analysis. Figure 14 and 15 show the results from TGA measurements and DSC, respectively. For the DSC results two data sets from different batches were averaged and for TGA one sample was prepared from each fraction. TGA analysis shows that the lignin is stable up until about 200 °C where it starts to degrade. The same trend can be seen from DSC where all samples enter a region of exothermic transitioning (i.e. degradation) at around 200 °C. The amount of material degrading varied between different samples. The EtOAc sample is the least thermally stable, likely due to it having the lowest molecular weight. The thermal stability increases with the molecular weight of the lignin fractions. Around 100 ℃ there is a small loss of weight that is due to evaporation of water and residual solvents in the lignin. Phenyl propane side groups are fragmented around the 100-300 ℃ range. The next range from 300 to 450 °C has the highest degree of degradation and is where the monomeric phenolic groups and some aromatic rings are degraded (Zhao and Liu, 2010).

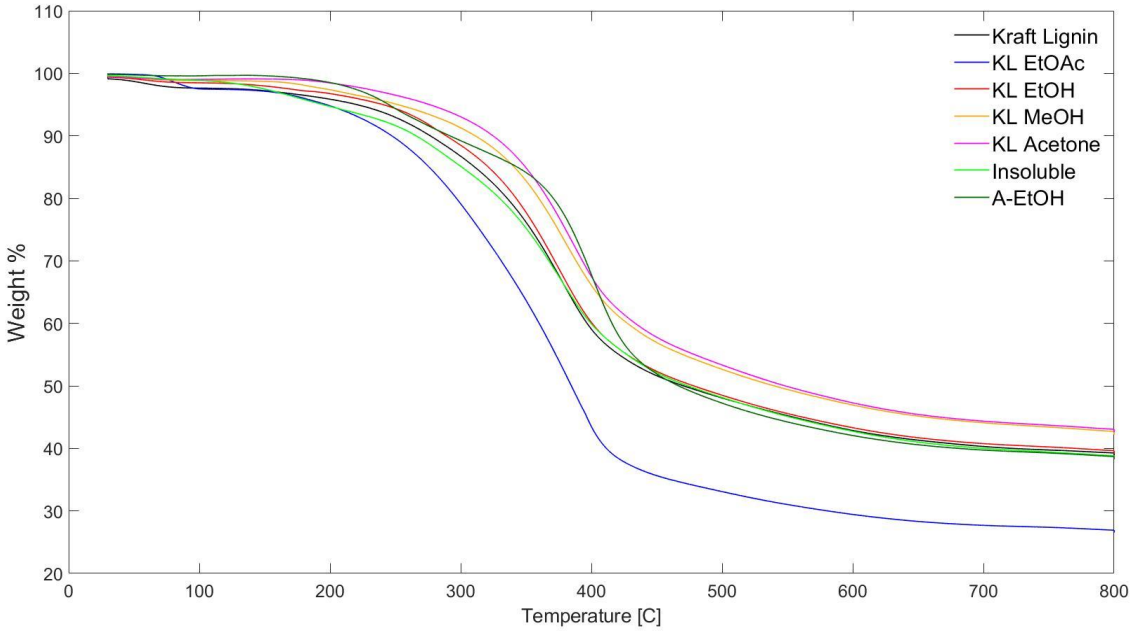

Figure 14. TGA results of Kraft lignin, all fractions, and the allylated EtOH fraction..

Solvent fractionated lignin shows a trend where T_g increases with increasing M_w. Longer chains have a higher degree of entanglement and less free volume, which increases stability and T_g. The trend is not linear, however, and the reason for this is because functional groups have an influence as well. A large content of hydroxyl functionalities will increase the degree

of hydrogen bonding that is going on, which will increase stability. However, the EtOAc fraction had the highest amount of hydroxyl content, and yet it still has the lowest T_g. This is because molecular weight affects more than hydroxyl content does (Park et al., 2018).

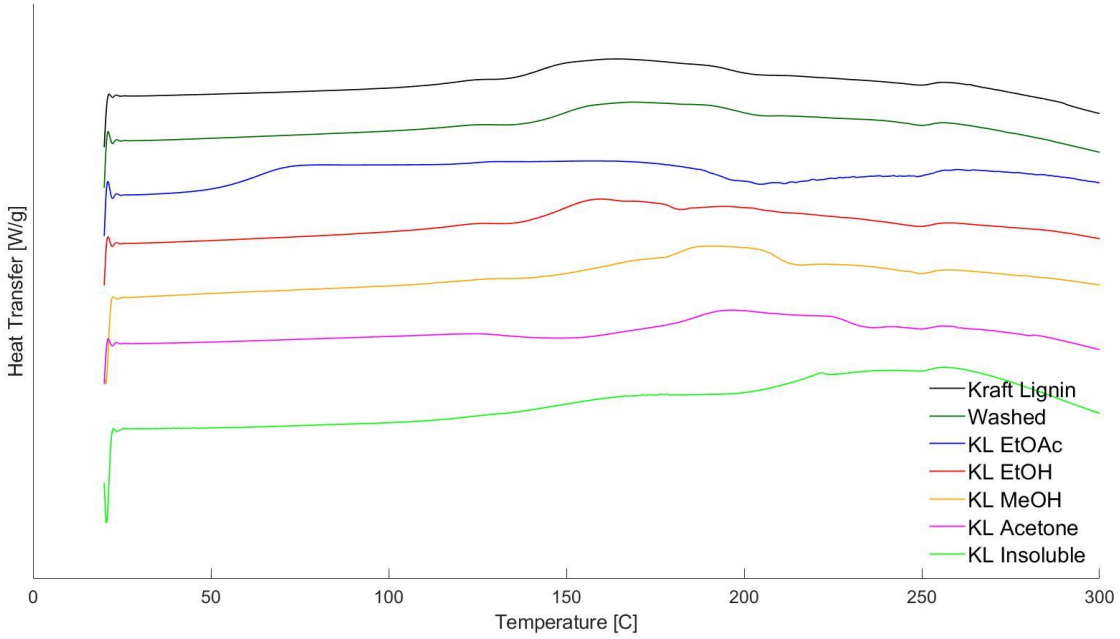

Figure 15. DSC results of Kraft lignin, washed lignin and all fractions.

4.1.5 Functional Groups

The spectra in Appendix C can be used as a reference for initial lignin. Lignin samples were analyzed with ATR FTIR and the results are presented in Figure 16. From these spectra, lignin's signature signals can be analysed and attributed to various functional groups. Table 3 below shows the attribution of signals to functional groups found in lignin (Bock and Gierlinger; Boeriu et al.; Ibrahim et al.; "IR Spectrum Table & Chart", Kubo and Kadla, 2005).

Table 3. IR vibrational frequency assignment for washed Kraft lignin.

Frequency range [cm^{-1}]	Vibration type	Frequency range [cm^{-1}]	Vibration type	Frequency range [cm^{-1}]	Vibration type
3550-3050	O-H stretch	1460	C-H deformation	1142	C-H
2932	C-H stretch	1421	Aromatic ring str.	1125	Aromatic C-H bend
2843	C-H stretch	1365	Phenol	1029	C-O , C-H
1709	C=O stretch	1265	C-O	965	C-H wagging
1595	Aromatic ring str.	1212	C-O	854	C-H plane deformation
1512	Aromatic ring str.	1152	C-H plane deformation	815	C-H plane deformation

Important peaks are marked with a vertical line along with their respective wavenumber. The range between 2700 cm^{-1} to 1800 cm^{-1} has been omitted since there are no signals there except for the low level signals arising from the diamond crystal between 2300 cm^{-1} and 1800 cm^{-1} .

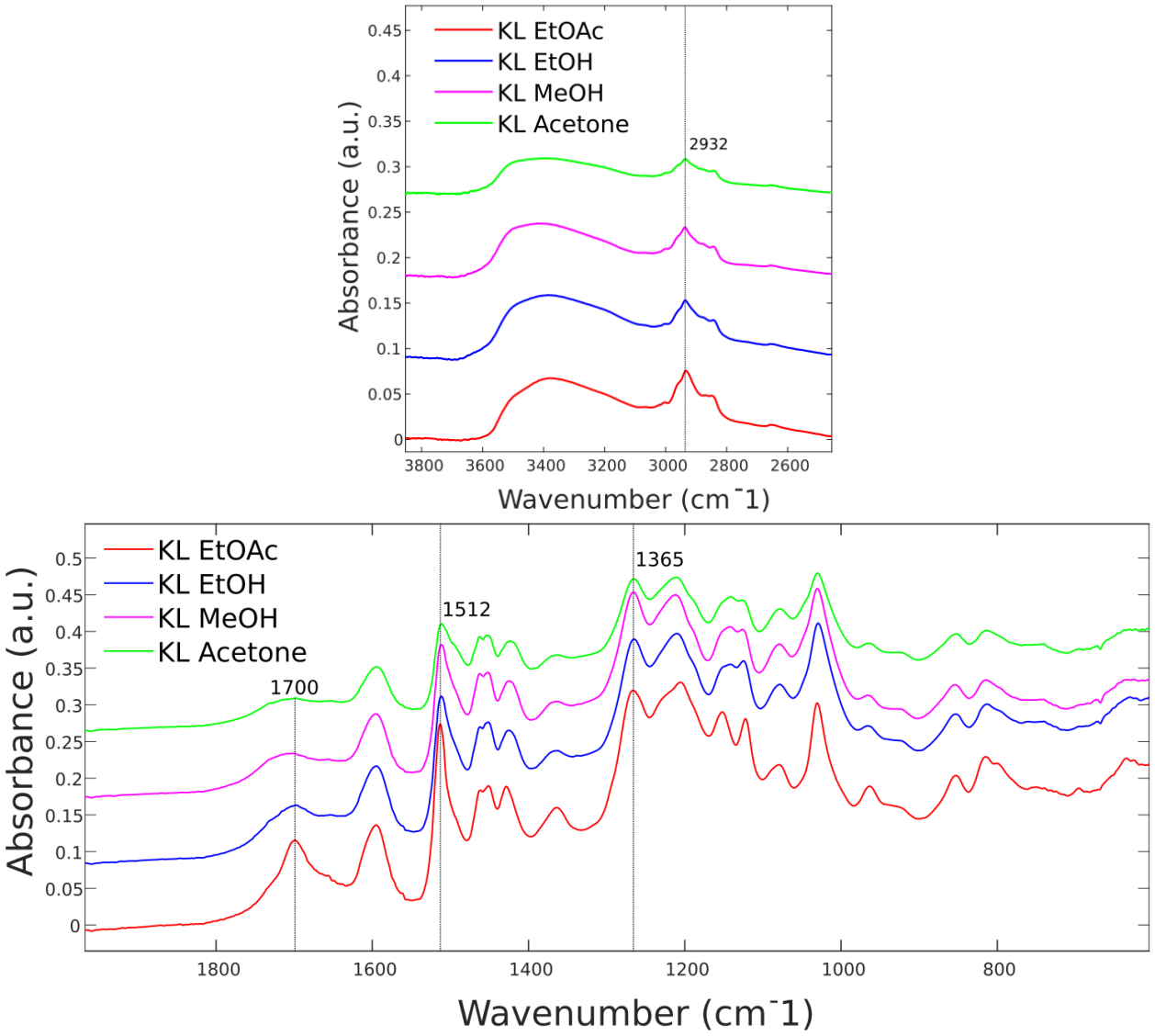

Figure 16. ATR FTIR spectra for Kraft lignin fractions soluble in EtOAc, EtOH, MeOH, Acetone.

Analysis of both ranges in Figure 16 reveals that most of the peaks present do not change in character while going through the fractionation process but rather gradually decrease in intensity. This can be seen clearly at peaks located at 2932 cm^{-1} , 1700 cm^{-1} , 1512 cm^{-1} and 1365 cm^{-1}.

4.2 Selective Allylation of the Ethanol Soluble Fraction

This section will present the results collected regarding the allylated ethanol fraction. The EtOH fraction was chosen for further modification because of its low M_w, high yield, and good solubility in the reaction media. The allylated lignin was analysed with SEC, TGA, DSC, ^{1}H-NMR, ^{31}P-NMR, FTIR and SEM.

4.2.1 Allylation Reaction

The success of the selective allylation reaction was assessed through ^{1}H-NMR, where the allyl functionality is expressed as three signals, ranging between 4.0 to 6.5 ppm on the spectra, as seen in figure 17. The EtOH fraction is included as well to visualize the forming of the new functional group. The two signals in the region 2-3 ppm are correlated to the water and deuterated solvent, and the signal at signal at 3.8 ppm was assigned to the methoxy group (Over and Meier, 2016). The molecular weight of the allylated lignin increased from 1800 to 1900 g/mol compared to the EtOH fraction, which was to be expected because of the added allyl functionalities. The dispersity was increased only somewhat, both for the low and high molecular weight regions. Any significant degradation losses can therefore be excluded.

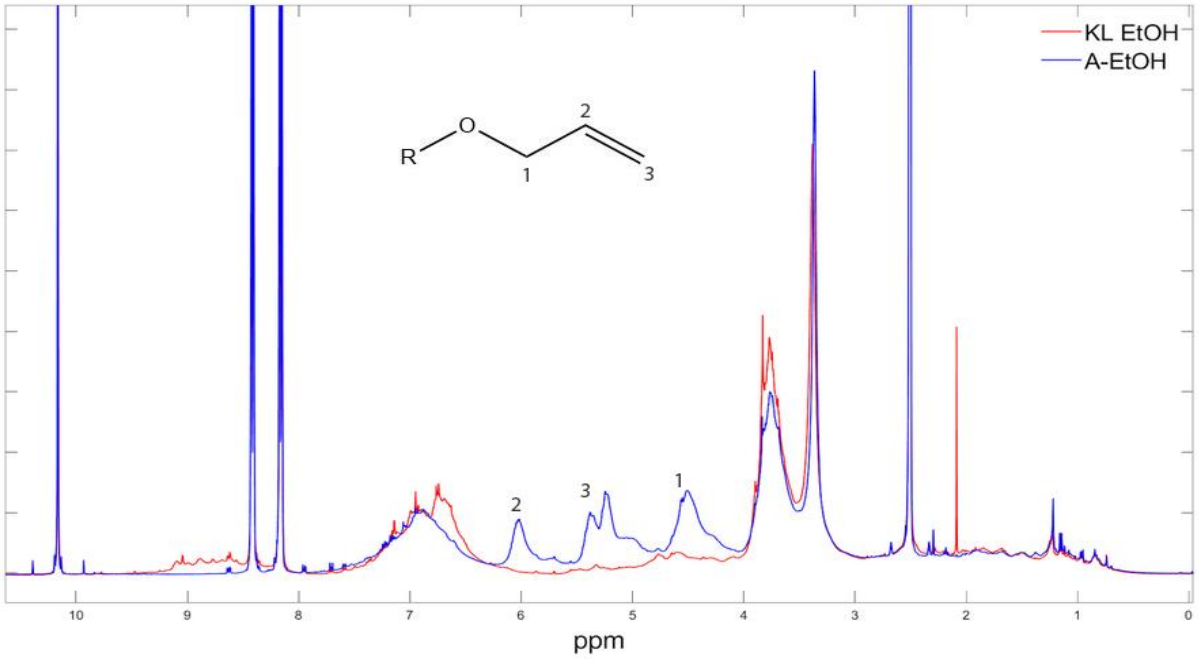

Figure 17.^{1}H-NMR of EtOH fraction and allylated lignin.

Selective allylation of phenolic hydroxyl groups could be additionally verified by ATR-FTIR analysis. A comparison between the ethanol fraction before allylation and after is presented in Figure 18. The area attributed to the phenolic and aliphatic hydroxyl groups of 3550 cm^{-1} to 3050 cm^{-1} is markedly smaller for the allylated lignin than for the unmodified ethanol soluble lignin. This is to be expected as a consequence of the allylation reaction since a high percentage of phenolic hydroxyl groups are reacted and their signal decreases. Another peak that corresponds to the phenolic group is found at 1367 cm^{-1} for the ethanol soluble lignin, this peak is greatly reduced in the spectrum for the allylated lignin. A small peak is present at 3078 cm^{-1} for the allylated lignin, this peak correlates to an allyl ether signal which is also expected. Other peaks that are present in the allylated lignin spectra but not the ethanol soluble lignin that can be assigned to the allyl group are located at 1647 cm^{-1}, 989 cm^{-1}, and 924 cm^{-1} (Socrates and Wiley).

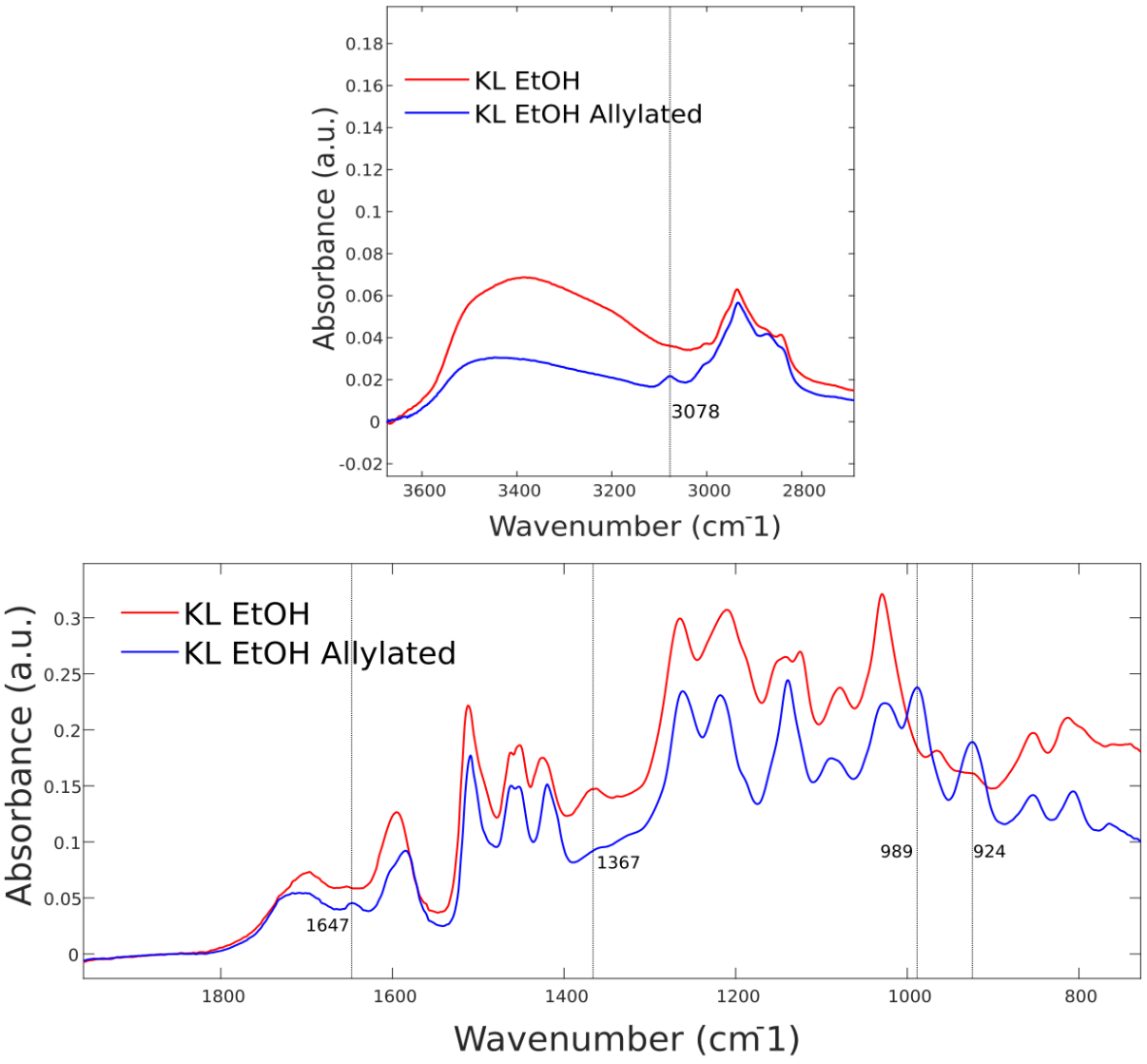

Figure 18. ATR-FTIR spectra of EtOH fraction and allylated lignin.

4.2.2 Hydroxyl Content

The hydroxyl content was quantified through ^{31}P-NMR and Figure 19 shows the spectra of the EtOH fraction and allylated lignin to visualize the change in functional group content. In the phenolic region there is a decrease, whilst the aliphatic and carboxylic functionalities stay roughly the same, indicating that the allylation is indeed highly selective. The conversion rate of allylated EtOH fractionated lignin was 3.69 ± 0.35 mmol of allyl functionality per gram of lignin, calculated as an average of 6 batches, which corresponds to an 82% reaction yield. It should be noted that lignin is highly heterogeneous and that different batches as received from the supplier can yield varying results.

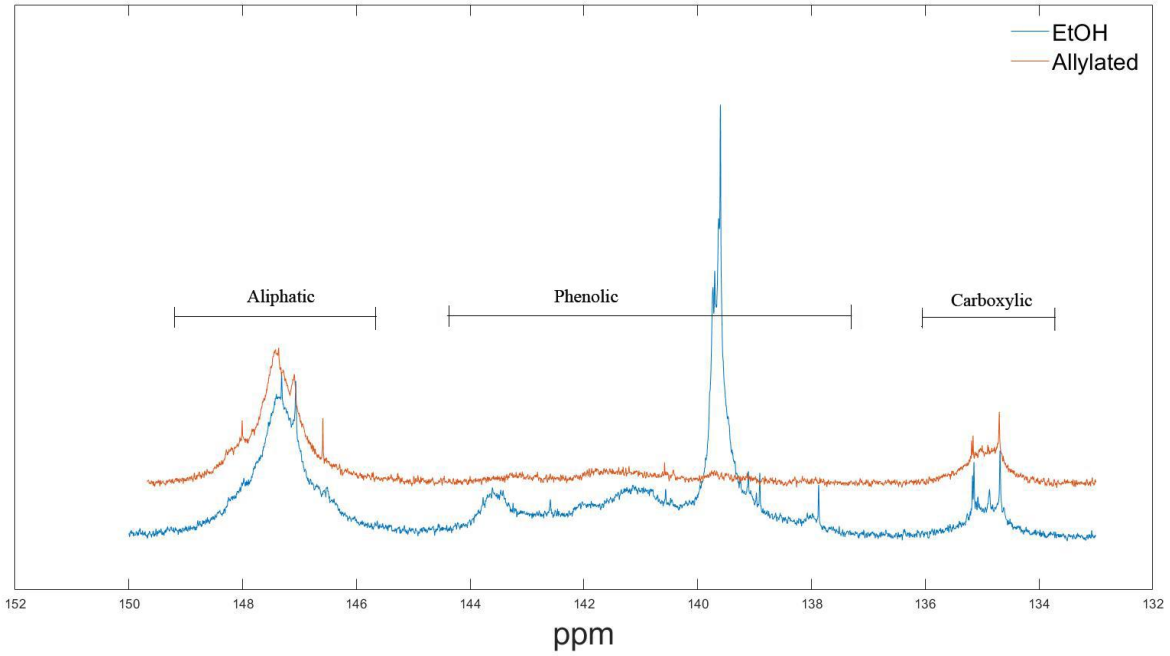

Figure 19. ^{31}P-NMR of EtOH fraction and allylated lignin.

4.2.3 Thermal Analysis

The thermal stability of the allylated lignin was concluded to be the same as for the other fractions, where degradation starts at around 200 ºC, see Figure 14 about TGA analysis in section 4.1. The DSC results of the EtOH fraction and allylated lignin are presented in Figure 20. The allylated lignin yields a different curve from the solvent fractionated lignin, with a noticeable exothermic peak. It also undergoes a glass transition in the region of 60-110 ºC. The T_g is lower than that of the EtOH fraction, which can be explained by how the allylated lignin has significantly lower hydroxyl content, and only slightly higher M_w (Park et al.,

2018). The exothermic peak could be indicating that the lignin is reacting in some way and a possible pathway is the Claisen rearrangement as studied on allylated lignin by Zoia et al. 2014. At the same time there is a large baseline shift which means that the sample could be decomposing as well (Thomas, n.d). This makes it clear that any processes conducted at too high of a temperature could be detrimental to the material because of potentially lost functional groups.

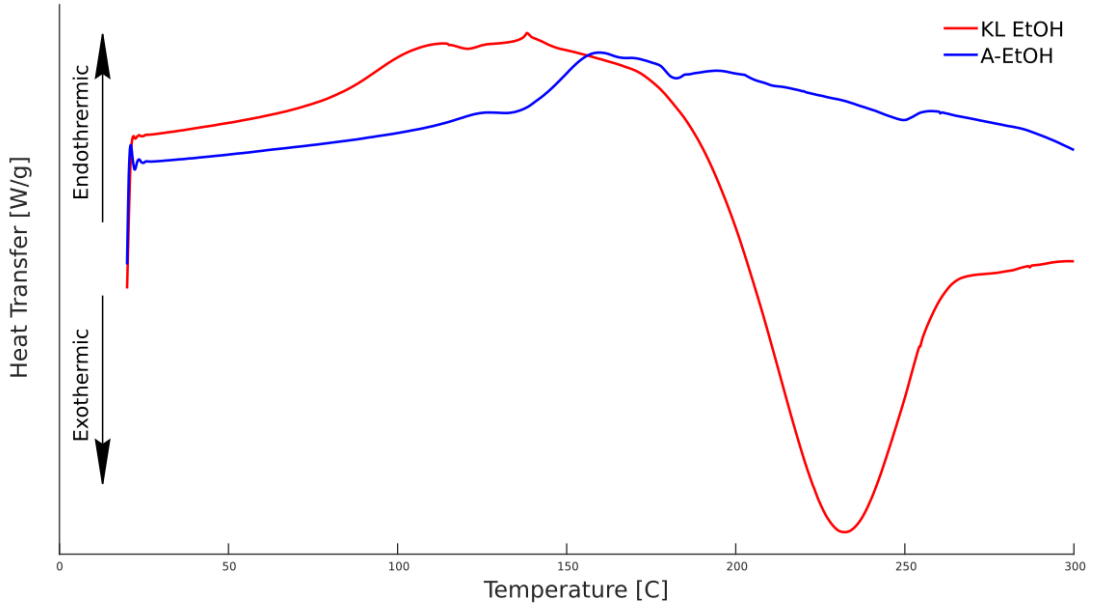

Figure 20. DSC results of EtOH fraction and allylated lignin

4.2.4 Morphology

Lignin morphology was investigated for unprocessed Kraft lignin, EtOH fraction, and the allylated lignin. SEM images showing typical morphologies for these different fractions can be seen in Figure 21.

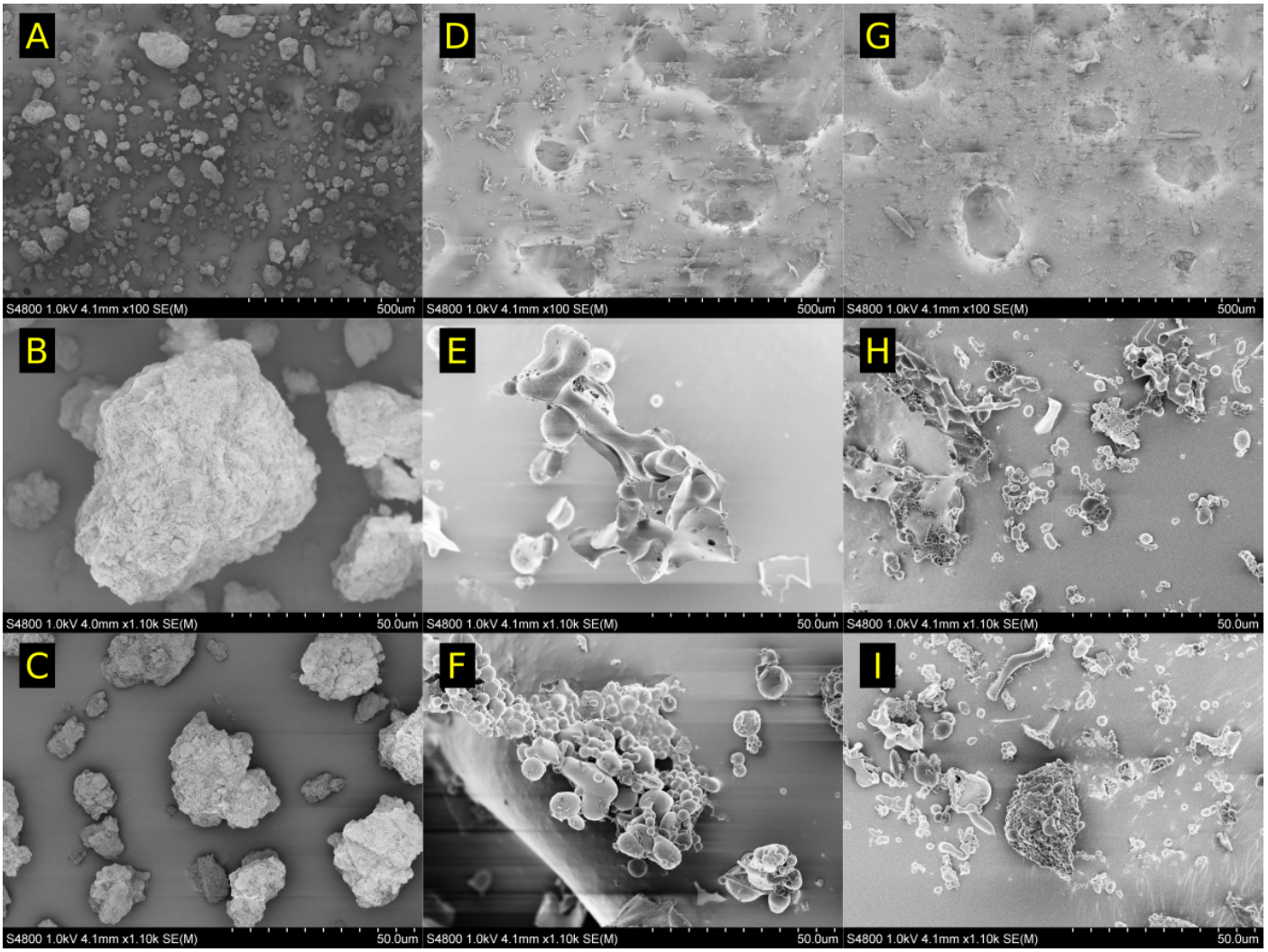

Figure 21. SEM images of unprocessed Kraft lignin (A,B,C), the EtOH fraction (D,E,F) and the allylated lignin (G,H,I).

By inspection of Figure 21 it is apparent that unprocessed Kraft lignin has a larger particle size than that of the ethanol soluble or allylated fraction. This size disparity can be attributed to the preparation through gradual precipitation, and freeze-drying, of the two latter fractions.

Observing the morphology of lignin is instructive and gives insight into how the heterogeneous macromolecule looks at a very fine scale, however the morphology has little impact on further processing as the lignin loses it's defined morphology when dissolved in solvent which is done in all processing steps except for washing of unprocessed Kraft lignin with water. Denser morphologies for processed fractions could conceivably affect solvation rate, this could be a contributing factor as to why certain batches of allylated lignin took longer to bring into solution.

4.3 Cross-Linking and Thermosetting of Composites

The results from the thermosetting of the composite materials will be summarized and discussed in this section. This includes the preparation of the resins, application to the carbon fibres as well as the curing process. The thermosetting reaction was analysed with FTIR and the composite materials were analysed with SEM. Multiple techniques were used on different samples in order to observe and evaluate the most successful method.

4.3.1 Cross-Linker Reaction

The consumption of allyl groups through the thiol-ene reaction could be verified with ATR FTIR. The spectra corresponding to uncured resin and cured resin are presented in Figure 22. The previously identified peaks attributed to the allyl group at 3078 cm^{-1}, 1647 cm^{-1}, 989 cm^{-1} and 924 cm^{-1}which are present for the resin before curing are significantly diminished for the cured resin, confirming the successful reaction of thiol and allyl groups. A further confirmation of this reaction is found in the diminishing of the thiol signal at 2569 cm^{-1}in Figure 22, indicating that much of the thiol cross-linker has been consumed (Nyquist, 2001; Ribca et al., 2021).

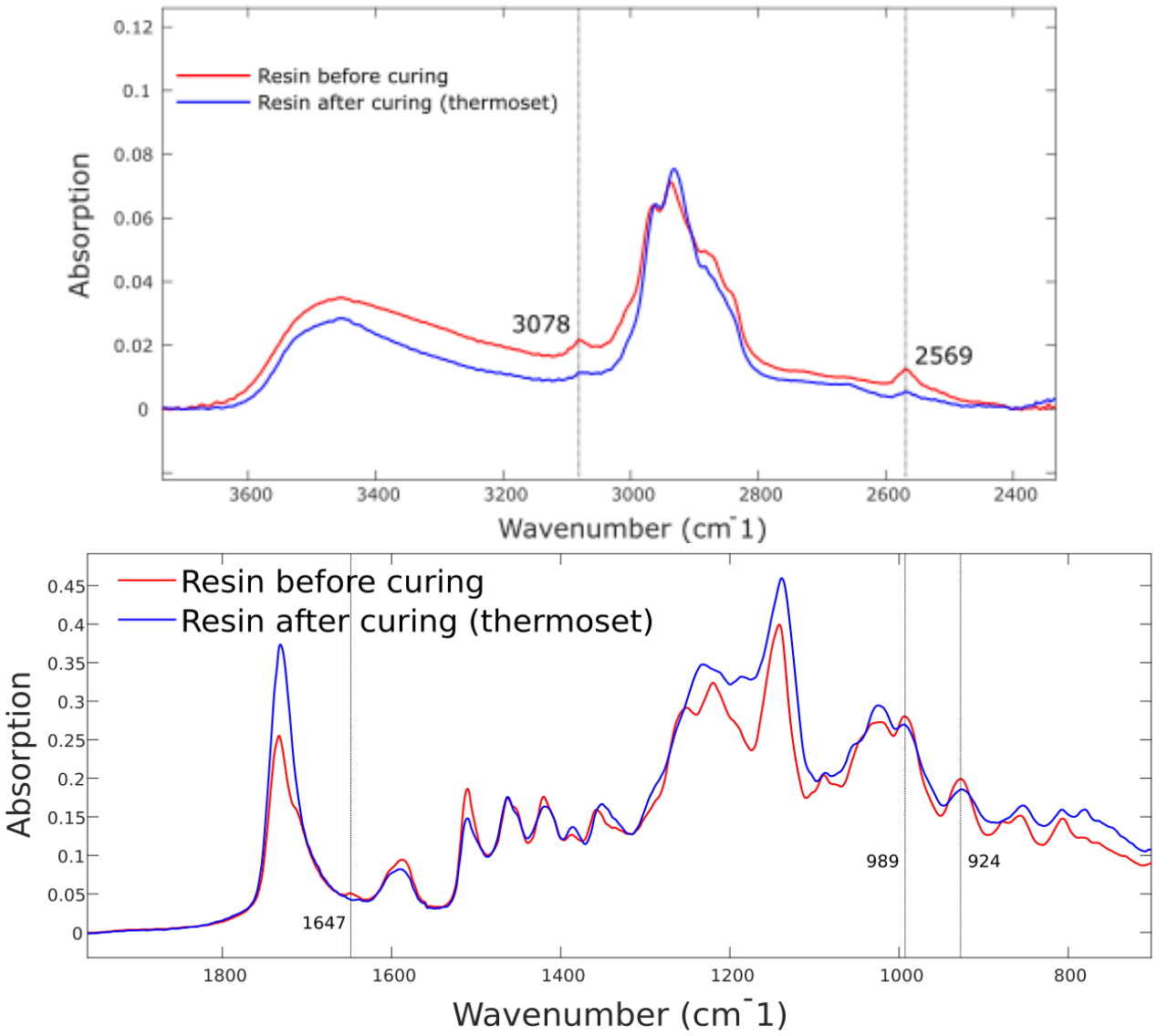

Figure 22. ATR FTIR spectra of uncured allylated lignin resin and cured allylated lignin resin (thermoset).

4.3.2 Preparation of Composites

A major problem with procuring the composites was the formation of gas bubbles. This defect was caused by the evaporation of the solvents. When the solvents were let to evaporate at a fast pace, more bubbles appeared at the surface of the composite. As a consequence, the carbon fibre was not fully covered and the impregnation was incomplete. The desired result would have been that the whole carbon fibre became well impregnated with the resin, with no

bubbles. To achieve this some different solvent mixtures of acetone and ethanol were tested with different ratios, with the best results stemming from a 1:2 - ethanol:acetone ratio.

The composites were heated stepwise up until 125 ºC and some batches were maintained at set temperatures for elongated or shortened periods of times. This was done in an effort to see at which rate the bubbles formed in the resin during heating and curing. In the end, however, forced rapid evaporation was fruitless, and to reach complete curing a temperature of 125 ºC was required to be maintained overnight. Some samples were also flipped half-way through curing. This resulted in glossy surfaces for what had previously been the bottom surface, but incomplete coverage of the top-side. Figures 23 and 24 show two images of what this looked like.

Figure 23. Flipped CF top-side, (previously bottom).

Figure 24. Flipped CF bottom surface, (previously top-side).

Another variable that was tested to improve the impregnation of the CF was to add pressure to the composites during curing. This resulted in spread out resin and incomplete coverage of the CF. Figure 25 shows what a pressed composite looked like. The top and bottom layers looked similar. Figure 26 shows the same composite but with back-light to display the issue of very little resin between the carbon fibre bands within the mat structure. In addition to having poorer looks, the pressed composite was thinner due to the resin floating out during compression and heating, which induces a viscosity drop.

Figure 25. Pressed composite

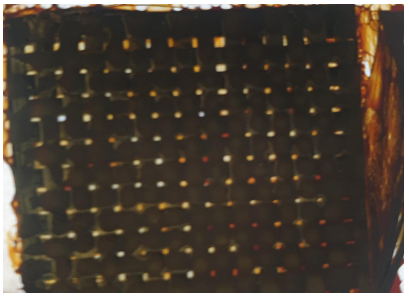

Figure 26. Pressed composite with back-light.

4.3.3 Adhesion of Resin to Carbon fibre

As a point of reference, SEM images were taken of the unmodified carbon fibre mat used to make composites in this study. These images are presented in Figure 27. The carbon fibres have a relatively smooth surface and have in the case of this carbon fibre mat a diameter between 6 µm and 9 µm.

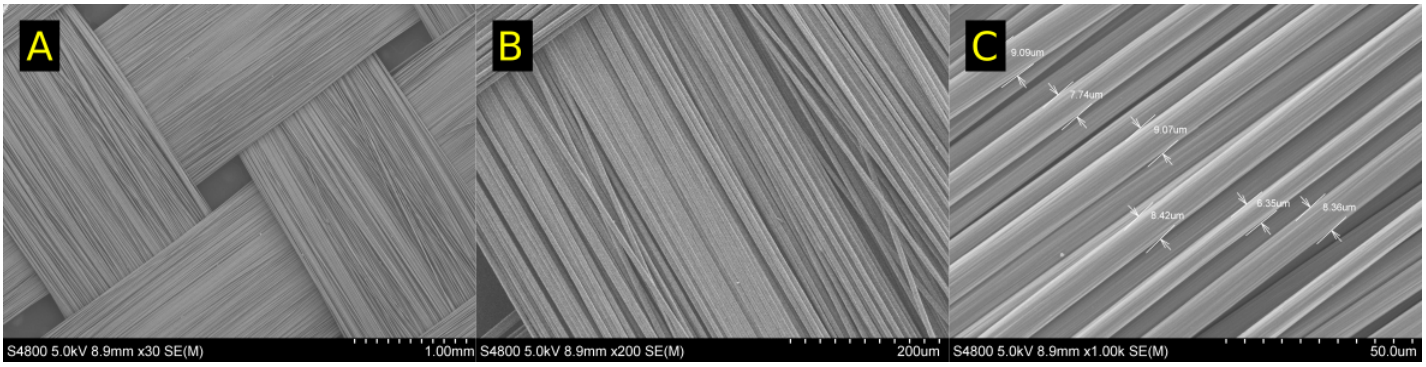

Figure 27. SEM images of carbon fibre mat and close up of carbon fibres.

The degree of impregnation, as well as resin adhesion to carbon fibres for the created composites was investigated with SEM. All images in Figure 28 show composites that have been compressed during the curing process. Figure 28.A shows a representative overview of what a top view of a cross section looks like. Resin can be observed coating the carbon fibres. The presence of resin on carbon fibres is seen in more detail in Figure 28 image B and E where E is a zoomed in portion of image B. In image E, resin can be seen adhering on and between carbon fibres; this leads to the conclusion that good impregnation has been achieved with the compressed composite.

Figure 28.C,F shows a top down view of vertical fibres in the cross section, There are no visible dark rings/gaps around the fibres, indicating that there is good adhesion between resin

and fibre. Most carbon fibre strands are snapped rather than just pulled out from the resin matrix, further proving the good adhesion characteristics present between resin and carbon fibre. Image D in Figure 28 shows another cross section where both the horizontal and vertical carbon fibre strands are visible, resin can be seen on the horizontal section and a geometry similar to that seen in image C is noted for the vertical area. At the boundary between the horizontal and vertical strands there are more dark spots which could be interpreted as areas where carbon fibres have dislodged and been pulled out. It could also be fibres that are broken but slightly further down which makes the area much darker in comparison. This sort of effect can be seen in images C and F in Figure 28.

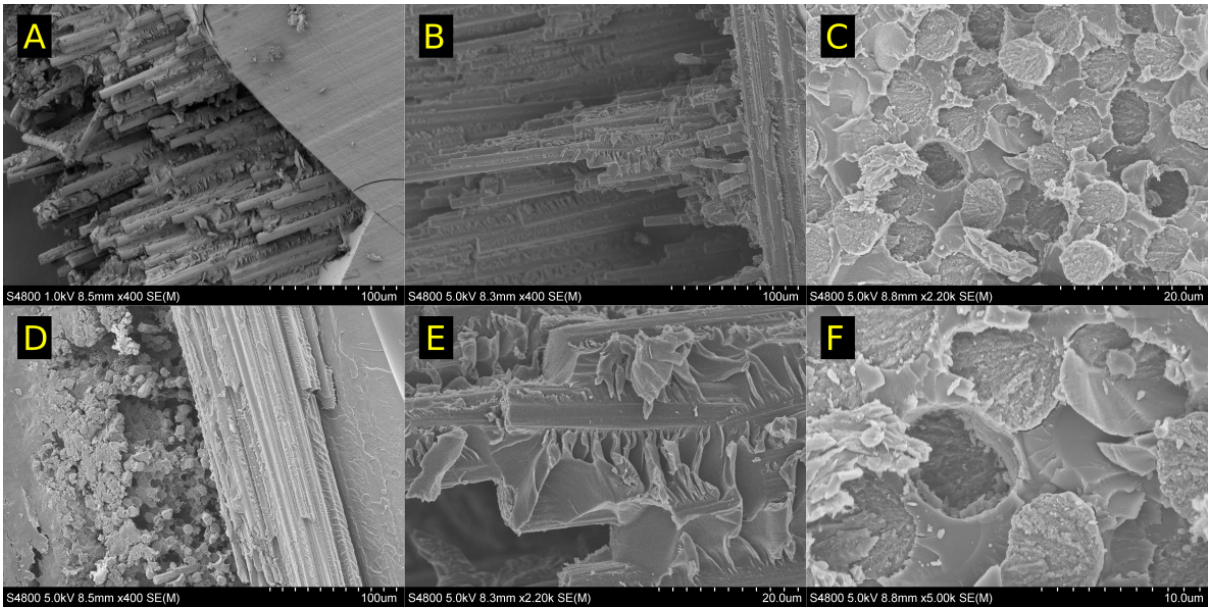

Figure 28. SEM images of cross sections of composites subject to compression during curing.

Composite samples which were cured without applied external pressure are shown in Figure 29. Unpressed composite samples show a lower degree of resin impregnation as evident by the many uncoated carbon fibre strands that stand out individually in Figure 29,A,C,E. The applied resin seems to have pooled at the top and bottom of the composite while leaving the middle of it bare, this is particularly visible in images D and E in Figure 29. Where the resin does impregnate the carbon fibre mat there is good adhesion between resin and carbon fibre comparable to that of the compressed samples, images D and F in figure 29 exemplify this observation.

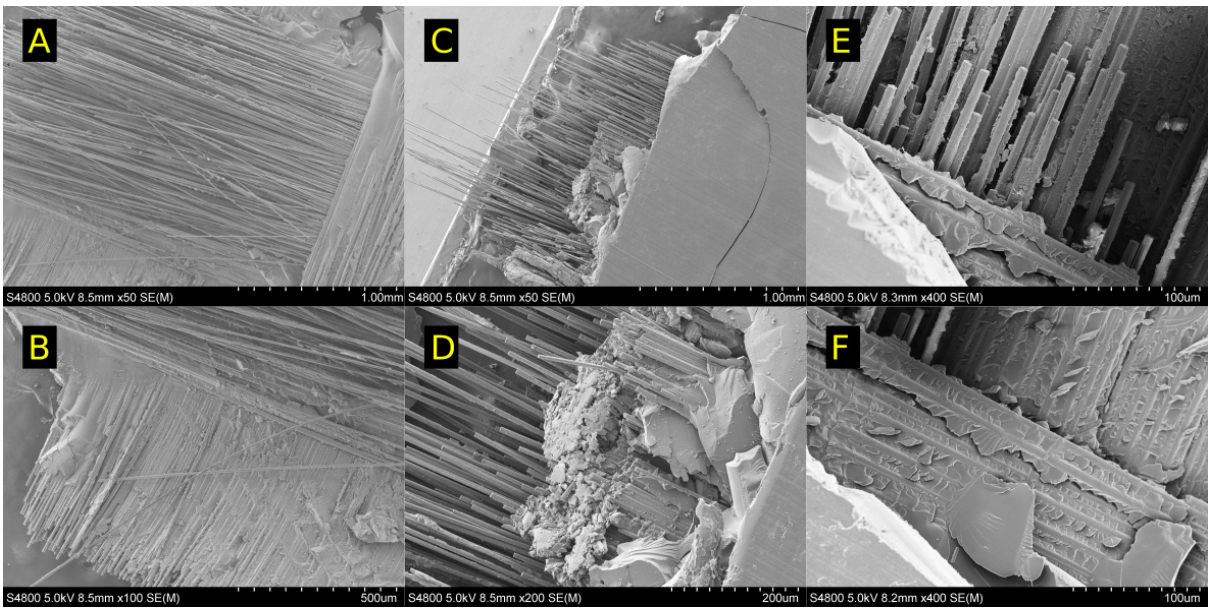

Figure 29. SEM images of composites cured without any applied external pressure. Images on the bottom row are magnified areas of the corresponding image on the top row.

A combination of curing with and without pressure is suggested as a possible pathway to obtain composites with good coating throughout the carbon fibre. First a layer of resin could be added to the carbon fibre mat and pressed in a hot press for some time. After the initial step another layer of resin could be applied, now without added pressure, to obtain the even and glossy finish and adequate resin to carbon fibre ratio.

5. Conclusions

Kraft lignin can be effectively solvent fractionated with the utilized solvents, in this report, namely ethyl acetate, ethanol, methanol and acetone. They are all classified as green solvents and can successfully extract fractions from lignin with varying molecular weights and functional group content. Fractions with low molecular weight and dispersity are achieved. The ethyl acetate and ethanol soluble fractions had the best yield and contained the highest content of hydroxyl functionality.

The ethanol soluble fraction was successfully allylated and allyl functionality was confirmed through ^{1}H-NMR. The conversion rate was quantified through assessing the change in phenolic hydroxyl content in the ethanol and allylated samples. Hydroxyl content was analysed with ^{31}P-NMR and also showed that the reaction was highly selective towards the phenolic hydroxyl groups. A conversion rate of 82% was achieved.

The resin was prepared by mixing allylated lignin with 3TMP and a 1:2 mixture of ethanol and acetone was used as a cosolvent. The resin was applied to 3x3 cm carbon fibre mats and were cured with and without applied pressure. The non-pressed composites had a glossy and appealing surface, but showed incomplete coverage of the mats because of air bubbles. The pressed composites lost some resin and as a consequence were thin and showed a lot of exposed carbon fibres.

The preparation of composites showed that adding pressure had a major positive impact on the penetration of the resin into the carbon fibre mat. Interfacial adhesion as investigated through SEM analysis was found to be good for the pressed samples.

Bubble formation was a problem for all samples prepared, whether it was during solvent evaporation or during curing. By performing the addition of resin to carbon fibre mats in multiple steps, where pressure is added after the first applied layer, it is suggested that complete adhesion to the carbon fibre can be achieved, whilst maintaining adequate resin to carbon fibre ratio.

References

Aminzadeh, S., Lauberts, M., Dobele, G., Ponomarenko, J., Mattsson, T., Lindström, Mikael E and Sevastyanova, O. (2018). Membrane filtration of kraft lignin: Structural characteristics and antioxidant activity of the low molecular weight fraction. *Industrial Crops and Products*, [online] 112, pp.200–209. Available at: https://www.sciencedirect.com/science/article/pii/S0926669017308014.

Auvergne, R., Caillol, S., David, G., Boutevin, B. and Pascault, J. (2014). Biobased Thermosetting Epoxy: Present and Future. *Chem. Rev.*, [online] 114(2), pp.1082–1115. Available at: https://doi.org/10.1021/cr3001274.

Bock, P. and Gierlinger, N. (2019). Infrared and Raman spectra of lignin substructures: Coniferyl alcohol, abietin, and coniferyl aldehyde. *Journal of Raman Spectroscopy*, [online] 50(6). Available at: https://doi.org/10.1002/jrs.5588

Boeriu, C.G., Bravo, D., Gosselink, R.J.A. and van Dam, J.E.G. (2004). Characterisation of structure-dependent functional properties of lignin with infrared spectroscopy. *Industrial Crops and Products*, [online] 20(2), pp.205–218. Available at: https://doi.org/10.1016/j.indcrop.2004.04.022

Bpf.co.uk. (2021). *Polymers: Thermosets*. [online] Available at: https://www.bpf.co.uk/plastipedia/polymers/default.aspx#:~:text=Furan-,Properties%3A,self%20extinguishing%2C%20low%20smoke%20emissions. [Accessed 17 May 2021].

Brodin, I., Sjöholm, E. and Gellerstedt, G. (2009). Kraft lignin as feedstock for chemical products: The effects of membrane filtration. *Holzforschung*, [online] 63, pp.290–297. Available at: https://doi.org/10.1515/HF.2009.049

Buono, P., Duval, A., Verge, P., Averous, L. and Habibi, Y. (2016). New Insights on the Chemical Modification of Lignin: Acetylation versus Silylation. *ACS Sustainable Chemistry & Engineering*, [online] 4(10), pp.5212–5222. Available at: https://doi.org/10.1021/acssuschemeng.6b00903

Cederholm, L., Xu, Y., Tagami, A., Sevastyanova, O., Odelius, K. and Hakkarainen, M. (2020). Microwave processing of lignin in green solvents: A high yield process to narrow dispersity oligomers. *Industrial Crops and Products*, [online] 145, p.112152. Available at: https://www.sciencedirect.com/science/article/pii/S0926669020300686.

Chung, H. and Washburn, N.R. (2016). Extraction and Types of Lignin. *Lignin in Polymer Composites*, pp.13–25. In book: Lignin in Polymer composites. doi: 10.1016/b978-0-323-35565-0.00002-3

Clayden, J., Greeves, N. and Warren, S.G. (2012). *Organic chemistry*. 2nd ed. Oxford ; New York: Oxford University Press, pp.909–910.

Compositesworld.com. (2016). *Materials & Processes: Fabrication methods*. [online] Available at: https://www.compositesworld.com/articles/fabrication-methods [Accessed 18 May 2021].

Crestini, C., Lange, H., Sette, M. and Argyropoulos, D. (2017). On the structure of softwood kraft lignin. *Green Chem.*, 19, pp.4104–4121. doi: 10.1039/C7GC01812F

Duval, A., Vilaplana, F., Crestini, C. and Lawoko, M. (2016). Solvent screening for the fractionation of industrial kraft lignin. *Holzforschung*, [online] 70(1), pp.11–20. Available at: https://www.degruyter.com/document/doi/10.1515/hf-2014-0346/html.

El Mansouri, N.-E., Farriol, X. and Salvadó, J. (2006). Structural modification and characterization of lignosulfonate by a reaction in an alkaline medium for its incorporation into phenolic resins. *Journal of Applied Polymer Science*, [online] 102(4), pp.3286–3292. Available at: [Accessed 24 Feb. 2021].

Frederick and Claude, H. (2005). An Extensive New Literature Concerning LowDose Effects of Bisphenol A Shows the Need for a New Risk Assessment. *Environmental Health Perspectives*, [online] 113(8), pp.926–933. Available at: https://doi.org/10.1289/ehp.7713 [Accessed 21 May 2021].

Gioia, C., Lo Re, G., Lawoko, M. and Berglund, L. (2018). Tunable Thermosetting Epoxies Based on Fractionated and Well-Characterized Lignins. *Journal of the American Chemical Society*, 140(11), pp.4054–4061. doi: 10.1021/jacs.7b13620

Henriksson, G., Li, J., Zhang, L. and Lindström, M.E. (2010). *Chapter 9:Lignin Utilization*. [online] pubs.rsc.org. Available at: https://pubs.rsc.org/en/content/chapter/9781849732260-00222/978-1-84973-226-0 [Accessed 21 May 2021].

Hoyle, C.E., Lee, T.Y. and Roper, T. (2004). Thiol-enes: Chemistry of the past with promise for the future. *Journal of Polymer Science Part A: Polymer Chemistry*, [online] 42(21), pp.5301–5338. Available at: https://onlinelibrary.wiley.com/doi/full/10.1002/pola.20366#bib5 [Accessed 20 May 2021].

Hoyle, Charles E. and Bowman, Christopher N. (2010). Thiol-Ene Click Chemistry. *Angewandte Chemie International Edition*, [online] 49(9), pp.1540–1573. Available at: https://onlinelibrary.wiley.com/doi/pdf/10.1002/anie.200903924?saml_referrer [Accessed 18 May 2021].

Hsissou, R., Seghiri, R., Benzekri, Z., Hilali, M., Rafik, M. and Elharfi, A. (2021). Polymer composite materials: A comprehensive review. *Composite Structures*, [online] 262(262), p.113640. Available at: https://www.sciencedirect.com/science/article/abs/pii/S026382232100101X [Accessed 7 May 2021].

Huang, J., Fu, S. and Gan, L. (2019). Structure and Characteristics of Lignin. *Chapter 2: Lignin Chemistry and Applications*, [online] pp.25–50. Available at: https://www.sciencedirect.com/science/article/pii/B9780128139417000023 [Accessed 8 May 2019]. From book: Lignin Chemistry and Applications.

Ibrahim, M.N.M., Iqbal, A., Shen, C.C., Bhawani, S.A. and Adam, F. (2019). Synthesis of lignin based composites of TiO2 for potential application as radical scavengers in sunscreen formulation. *BMC Chemistry*, 13(1). doi: 10.1186/s13065-019-0537-3

Jawaid, M., Thariq, M. and Naheed Saba (2019). *Mechanical and physical testing of biocomposites, fibre-reinforced composites and hybrid composites*. Duxford, United Kingdom Woodhead Publishing. ISBN: 9780081022924

Jawerth, M., Johansson, M., Lundmark, S., Gioia, C. and Lawoko, M. (2017). Renewable Thiol–Ene Thermosets Based on Refined and Selectively Allylated Industrial Lignin. *ACS Sustainable Chemistry & Engineering*, 5(11), pp.10918–10925. doi: 10.1021/acssuschemeng.7b02822

Jawerth, M.E., Brett, C.J., Terrier, C., Larsson, P.T., Lawoko, M., Roth, S.V., Lundmark, S. and Johansson, M. (2020). Mechanical and Morphological Properties of Lignin-Based Thermosets. *ACS Applied Polymer Materials*, 2(2), pp.668–676. doi: 10.1021/acsapm.9b01007

Jiang, X., Savithri, D., Du, X., Pawar, S., Jameel, H., Chang, H. and Zhou, X. (2017). Fractionation and Characterization of Kraft Lignin by Sequential Precipitation with Various Organic Solvents. *ACS Sustainable Chem. Eng.*, [online] 5(1), pp.835–842. Available at: https://doi.org/10.1021/acssuschemeng.6b02174.

Katahira, R., Elder, T.J. and Beckham, G.T. (2018). Chapter 1 A Brief Introduction to Lignin Structure. *pubs.rsc.org*, [online] pp.1–20. Available at: https://pubs.rsc.org/en/content/chapterhtml/2018/bk9781782625544-00001?isbn=978-1-78262-554-4&sercode=bk [Accessed 22 Feb. 2021]. From the book series: "Energy and Environment Series."

Komornicki, J., Bax, L., Vasiliadis, H., Magallon, I. and Ong, K. (2015). *Polymer Composites for Automotive Sustainability*. [online] Sustainable Chemistry. Available at: https://baxcompany.com/wp-content/uploads/2016/09/Suschem_Polymers_Brochure1.pdf [Accessed 11 May 2021].

Koo, S.P.S., Stamenović, M.M., Prasath, R.A., Inglis, A.J., Du Prez, F.E., Barner‐Kowollik, C., Van Camp, W. and Junker, T. (2010). Limitations of radical thiol‐ene reactions for polymer–polymer conjugation. *Journal of Polymer Science Part A: Polymer Chemistry*, [online] 48(8), pp.1699–1713. Available at: https://onlinelibrary.wiley.com/doi/full/10.1002/pola.23933?saml_referrer [Accessed 20 May 2021].

Kubo, S. and Kadla, J.F. (2005). Hydrogen Bonding in Lignin: A Fourier Transform Infrared Model Compound Study. *Biomacromolecules*, 6(5), pp.2815–2821. doi: 10.1021/bm050288q

Laurichesse, S. and Avérous, L. (2014). Chemical modification of lignins: Towards biobased polymers. *Progress in Polymer Science*, 39(7), pp.1266–1290. doi: 10.1016/j.progpolymsci.2013.11.004

Li, Y. and Sarkanen, S. (2002). Alkylated Kraft Lignin-Based Thermoplastic Blends with Aliphatic Polyesters. *Macromolecules*, 35(26), pp.9707–9715. doi: 10.1021/ma021124u

Liao, Y., Zhong, R., d'Halluin, M., Verboekend, D. and Sels, B.F. (2020). Aromatics Production from Lignocellulosic Biomass: Shape Selective Dealkylation of Lignin-Derived Phenolics over Hierarchical ZSM-5. *ACS Sustainable Chemistry & Engineering*, 8(23), pp.8713–8722. doi:10.1021/acssuschemeng.0c02370

LIQUID EPOXY RESINS DOW. (n.d.). [online] . Available at: http://nmt.edu/academics/mtls/faculty/mccoy/docs2/chemistry/DowEpoxyResins.pdf

Luca Zoia, Salanti, A., Frigerio, P. and Orlandi, M. (2014). Exploring Allylation and Claisen Rearrangement as a Novel Chemical Modification of Lignin. *BioResources*, [online] 9(4), pp.6540–6561. Available at: https://ojs.cnr.ncsu.edu/index.php/BioRes/article/view/BioRes_09_4_6540_Zoia_Allylation_Claisen_Rearrangement [Accessed 16 May 2021].

McIlhagger, A., Archer, E. and McIlhagger, R. (2015). Manufacturing processes for composite materials and components for aerospace applications. *Polymer Composites in the Aerospace Industry*, [online] pp.53–75. Available at: https://www.sciencedirect.com/science/article/pii/B9780857095237000037 [Accessed 21 May 2021].

Meng, X., Crestini, C., Ben, H., Hao, N., Pu, Y., Ragauskas, A.J. and Argyropoulos, D.S. (2019). Determination of hydroxyl groups in biorefinery resources via quantitative 31P NMR spectroscopy. *Nature Protocols*, [online] 14(9), pp.2627–2647. Available at: https://www.nature.com/articles/s41596-019-0191-1 [Accessed 19 May 2021].

Mohammad Armanmehr, Fatemeh Mohajer and Elham Khademloo (2013). Production of allyl chloride from chlorination of propylene. *Zenodo*. [online] Available at: https://zenodo.org/record/3594264#.YKDrrqgzZPY.

Over, L.C. and Meier, M.A.R. (2016). Sustainable allylation of organosolv lignin with diallyl carbonate and detailed structural characterization of modified lignin. *Green Chemistry*, 18(1), pp.197–207. doi: 10.1039/c5gc01882j

Pandey, K.K. (1999). A study of chemical structure of soft and hardwood and wood polymers by FTIR spectroscopy. *Journal of Applied Polymer Science*, [online] 71(12), pp.1969–1975. Available at: https://onlinelibrary.wiley.com/doi/full/10.1002/%28SICI%291097-4628%2819990321%2971%3A12%3C1969%3A%3AAID-APP6%3E3.0.CO%3B2-D?saml_referrer [Accessed 9 May 2021].

Park, C.H. and Lee, W.I. (2012). Compression molding in polymer matrix composites. *Manufacturing Techniques for Polymer Matrix Composites (PMCs)*, [online] pp.47–94. Available at: https://www.sciencedirect.com/science/article/pii/B9780857090676500031 [Accessed 21 May 2021].

Park, S.Y., Kim, J.-Y., Youn, H.J. and Choi, J.W. (2018). Fractionation of lignin macromolecules by sequential organic solvents systems and their characterization for further valuable applications. *International Journal of Biological Macromolecules*, 106(), pp.793–802. doi: 10.1016/j.ijbiomac.2017.08.069

Rajak, D.K., Pagar, D.D., Kumar, R. and Pruncu, C.I. (2019). Recent progress of reinforcement materials: a comprehensive overview of composite materials. *Journal of Materials Research and Technology*, 8(6), pp.6354–6374. doi: 10.1016/j.jmrt.2019.09.068

Ramezani Kakroodi, A., Kazemi, Y. and Rodrigue, D. (2013). Mechanical, rheological, morphological and water absorption properties of maleated polyethylene/hemp composites: Effect of ground tire rubber addition. *Composites Part B: Engineering*, [online] 51, pp.337–344. Available at: https://www.sciencedirect.com/science/article/pii/S1359836813001340?via%3Dihub [Accessed 21 May 2021].

Sameni, J., Krigstin, S., Rosa, D., Leao, A. and Sain, M. (2014). Thermal Characteristics of Lignin Residue from Industrial Processes. *Bioresources*, [online] 9, pp.725–737. Available at: https://www.researchgate.net/publication/262802756_Thermal_Characteristics_of_Lignin_Residue_from_Industrial_Processes [Accessed 9 Jun. 2021].

Sharma, A.K., Bhandari, R., Aherwar, A. and Rimašauskienė, R. (2020). Matrix materials used in composites: A comprehensive study. *Materials Today: Proceedings*, 21(21), pp.1559–1562. doi: 10.1016/j.matpr.2019.11.086

Shokuhfar, A. and Arab, B. (2013). The effect of cross linking density on the mechanical properties and structure of the epoxy polymers: molecular dynamics simulation. *Journal of Molecular Modeling*, [online] 19(9), pp.3719–3731. Available at: https://link.springer.com/article/10.1007/s00894-013-1906-9 [Accessed 17 May 2021].

Sigma-Aldrich. (2019). *IR Spectrum Table & Chart*. [online] Available at: https://www.sigmaaldrich.com/technical-documents/articles/biology/ir-spectrum-table.html.

Simmons, B.A., Loqué, D. and Ralph, J. (2010). Advances in modifying lignin for enhanced biofuel production. *Current Opinion in Plant Biology*, [online] 13(3), pp.312–319. Available at: https://www.sciencedirect.com/science/article/pii/S1369526610000191.

Socrates, G. and Wiley, J. (2015). *Infrared and Raman characteristic group frequencies : tables and charts*. Chichester Etc.: John Wiley & Sons Ltd. ISBN: 9780470093078

Stücker, A., Podschun, J., Saake, B. and Lehnen, R. (2018). A novel quantitative31P NMR spectroscopic analysis of hydroxyl groups in lignosulfonic acids. *Analytical Methods*, 10(28), pp.3481–3488. doi: 10.1039/c8ay01272e

Thermosetting polymer. (1997). *IUPAC Compendium of Chemical Terminology*.

Thomas, L.C. (n.d.). *Interpreting Unexpected Events and Transitions in DSC Results*. [online] TA Instruments. Available at: http://www.tainstruments.com/pdf/literature/TA039.pdf [Accessed 2 May 2021].

Tomani, P. (2010). The lignoboost process. *Cellulose Chemistry and Technology*, [online] 44, p. Available at: https://www.researchgate.net/publication/264842444_The_lignoboost_process [Accessed 17 May 2021].

Wan, J., Li, C., Bu, Z.-Y., Xu, C.-J., Li, B.-G. and Fan, H. (2012). A comparative study of epoxy resin cured with a linear diamine and a branched polyamine. *Chemical Engineering Journal*, [online] 188, pp.160–172. Available at: https://www.sciencedirect.com/science/article/pii/S1385894712001763 [Accessed 18 May 2021].

www.valmet.com. (n.d.). *Lignin extraction process*. [online] Available at: https://www.valmet.com/pulp/other-value-adding-processes/lignin-separation/lignoboost-process/#:~:text=LignoBoost%20is%20a%20patented%20extraction [Accessed 19 May 2021].

Zhao, S. and Abu-Omar, M.M. (2021). Materials Based on Technical Bulk Lignin. *ACS Sustainable Chemistry & Engineering*, 9(4), pp.1477–1493. doi: 10.1021/acssuschemeng.0c08882

Zhao, X. and Liu, D. (2010). Chemical and thermal characteristics of lignins isolated from Siam weed stem by acetic acid and formic acid delignification. *Industrial Crops and Products*, [online] 32(3), pp.284–291. Available at: https://www.sciencedirect.com/science/article/pii/S0926669010001172 [Accessed 21 May 2021].

Appendix

Appendix A

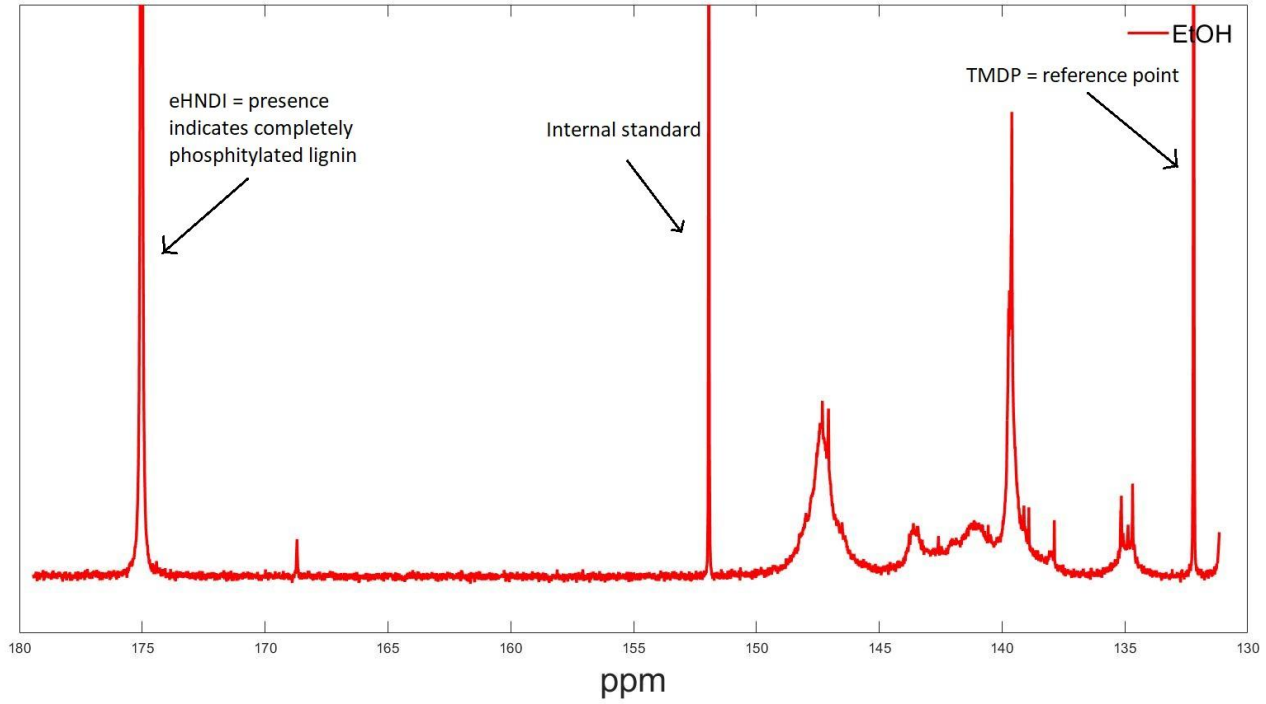

Appendix A. Entire ^{31}P-NMR spectra of EtOH fractionated lignin, displaying three important signals for the analysis of hydroxyl content in the samples.

Appendix B

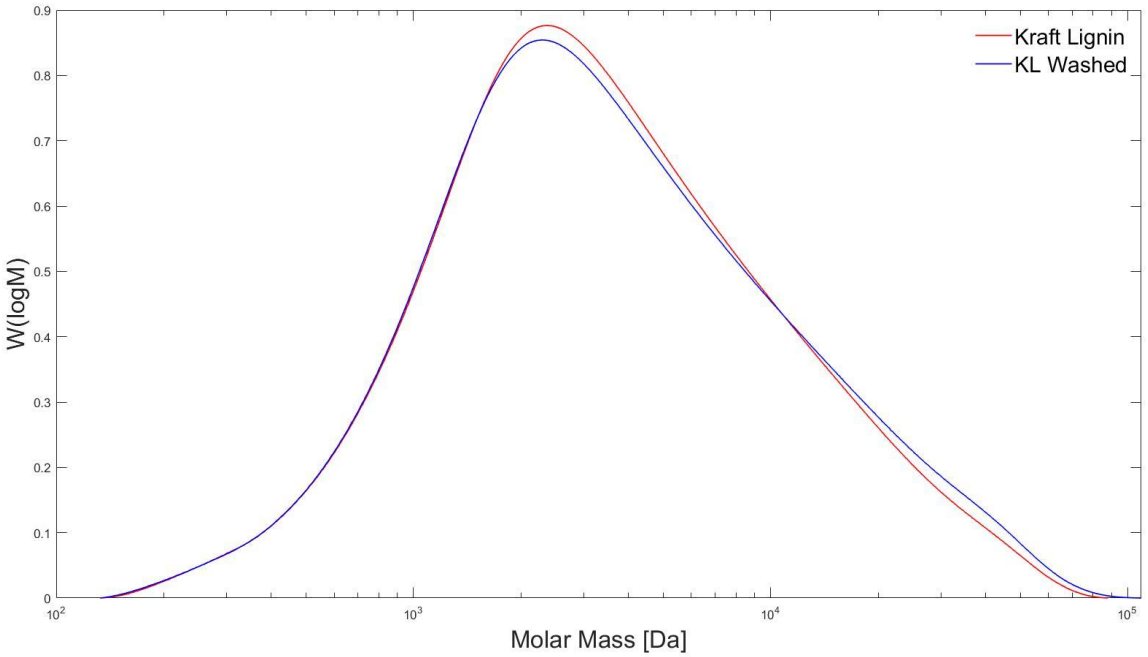

Appendix B. SEC results of Kraft lignin and washed lignin.

Appendix C

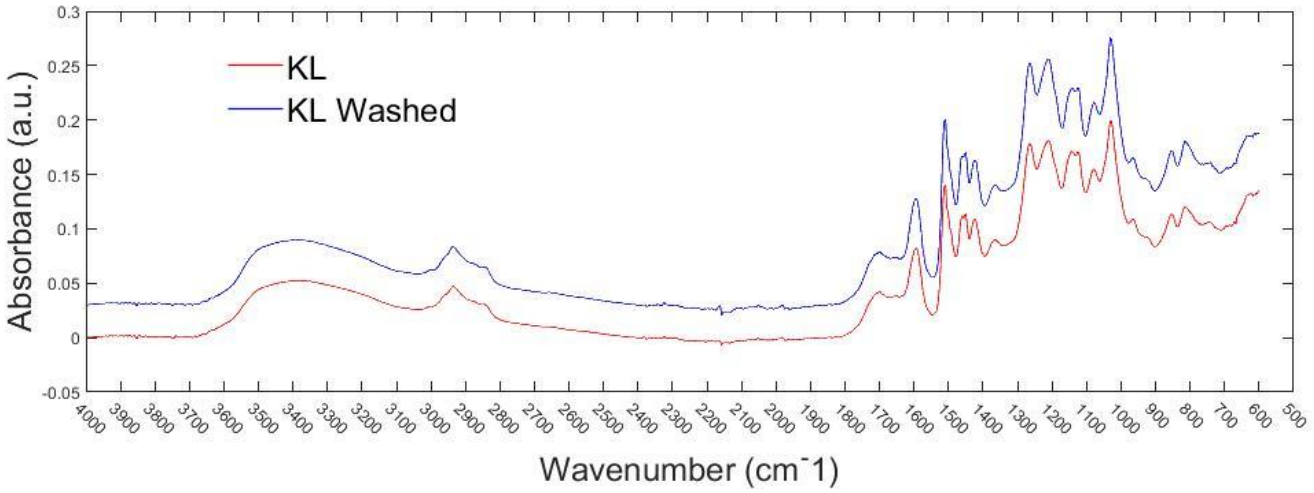

Appendix C. FTIR graphs of Kraft lignin and washed lignin.

Appendix D

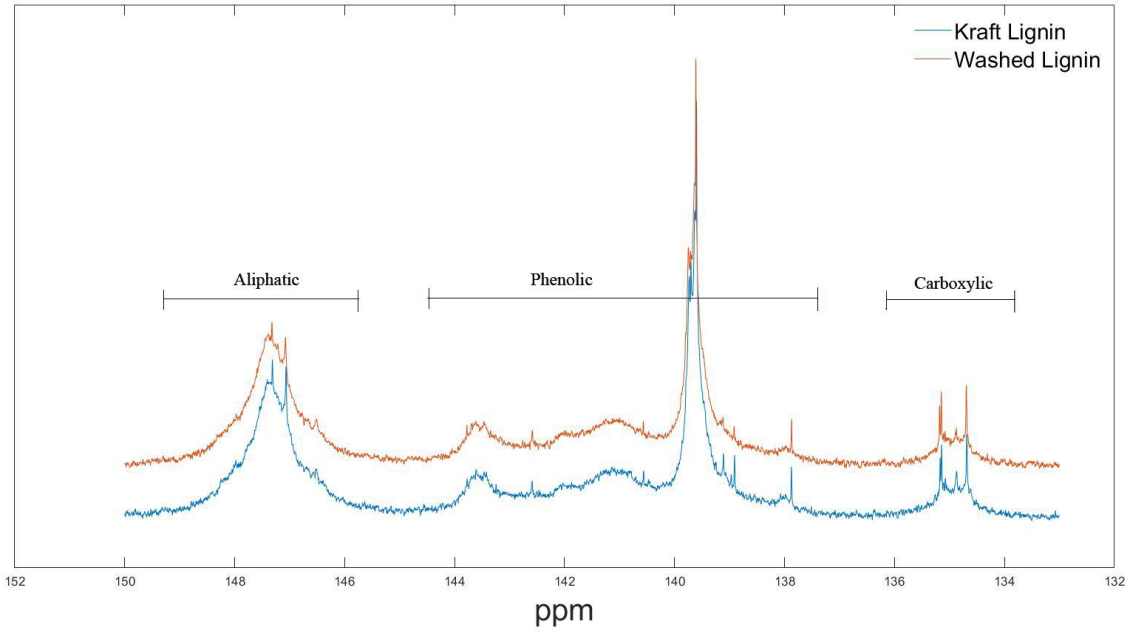

Appendix D. ^{31}P-NMR results of Kraft and washed lignin.

Appendix E

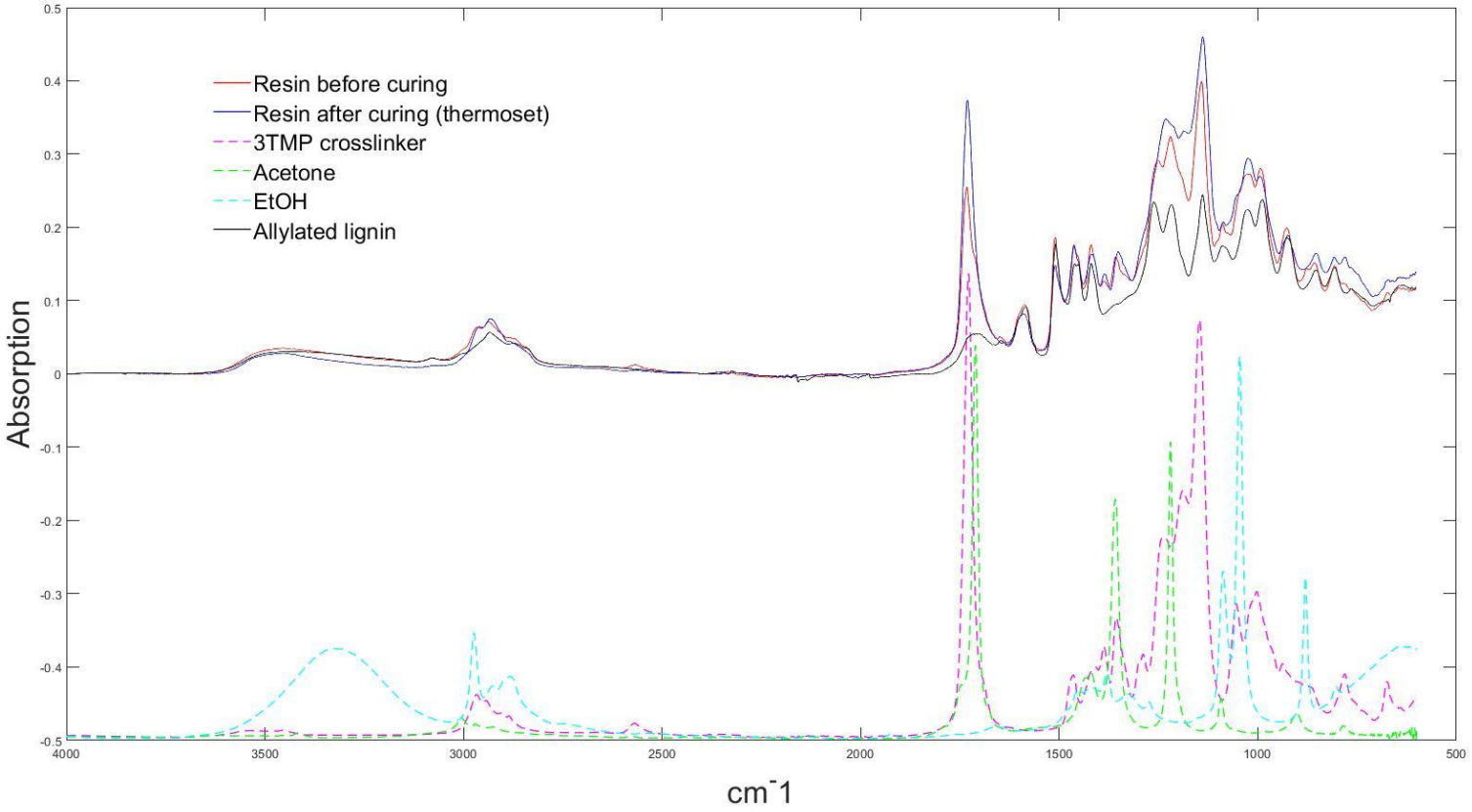

Appendix E. Resin, thermoset, allylated lignin, solvent and cross-linker signals